Electronic Supplementary Information (ESI)

Rituraj Das,[a] Dhrubajyoti Talukdar,[a] Plaban J. Sarma,[a] Hemrupa Kuilya,[b] Ranjit Thakuria[c], Diganta Choudhury*[b] and Sanjeev P. Mahanta*[a]

[a]Department of Chemical Sciences, Tezpur University, Tezpur, Assam, India.

[b]Department of Chemistry, B. Borooah College, Guwahati - 781007, Assam, India.

[c]Department of Chemistry, Gauhati University, Guwahati - 781014, Assam, India.

Email: digantachoudhury2008@gmail.com, spm@tezu.ernet.in

Colorimetric detection of fluoride ion in aqueous medium by thiourea derivatives: a transition metal ion assisted approach

General Methods

Instrumentation and reagents: All reagents and solvents were obtained from commercial sources and used as received, without further purification. All tetrabutylammonium salts for anion screening experiments were purchased from Sigma-Aldrich® and used as such. Infrared spectra were recorded with a Perkin Elmer Frontier MIRFIR spectrometer.

HRMS data were recorded by electron spray ionization with a Q-TOF mass analyzer. The electrospray ionization mass spectrometry (ESI-MS) spectrum of the receptors was recorded in methanol in Shimadzu-LCMS-2010 mass spectrometer. The ^{1}H NMR spectra (400 MHz) and ^{13}C NMR spectra (100 MHz) were recorded on a 'JEOL' NMR spectrophotometer in DMSO-d_6 at room temperature. In NMR spectra, chemical shifts are reported in parts per million (ppm) downfield of Me_4Si (TMS) as internal standard. EPR analysis was carried out with JEOL, Model: JES-FA200 spectrometer. 2D-NMR experiments (COSY, NOESY, HSQC, HMBC NMR) were performed in a 'Bruker' 600 MHz NMR spectrophotometer.

Cyclic Voltammogram and Differential Pulse Voltammetry (DPV) were done using Bio-Logics SP-300 with EIS facility. UV-Vis experiments were performed with Shimadzu UV-2550 spectrophotometer. UV-Vis titrations were carried out in dimethyl sulfoxide solution. The receptor solutions were titrated by adding known quantities of concentrated solution of the anions in question. Cyclic voltammetry experiments were carried out in a standard three electrode apparatus with a platinum working electrode, Ag/Ag^{+} (0.01 M $AgNO_3$ in 0.1 M TBAP in DMSO) reference electrode, and a Pt wire auxiliary electrode. The supporting electrolyte is 0.1 M tetrabutylammonium perchlorate (TBAP) in DMSO solution. The cell was maintained oxygen-free by purging dry nitrogen through the solution.

The limit of detection (LOD) value was calculated based on the anion titration of the developed probe under two conditions. To determine the S/N ratio, the absorbance of **C2** without the ion, F^{-} was measured upto ten times and the standard deviation of blank measurements was determined. Similarly, to determine the S/N ratio presence of the metal ion, the absorbance of **C2**.Ni^{2+}/Cu^{2+} mixture without the presence of F^{-} was measured ten times and the value was calculated. So the detection limit of **C2** and **C2**.Ni^{2+}/Cu^{2+} for F^{-} were determined from the following equation: $LOD = K \times S_b/S$ Where K = 2 or 3 (we take 2 in this case); S_b is the standard deviation of the blank solution; S is the slope of the calibration curve.[1] The fluoride contaminated groundwater samples collected from Baghpani village (Coordinates: 26.286372, 93.001249), Karbi Anglong, Assam, India was used as such

Synthesis and characterization

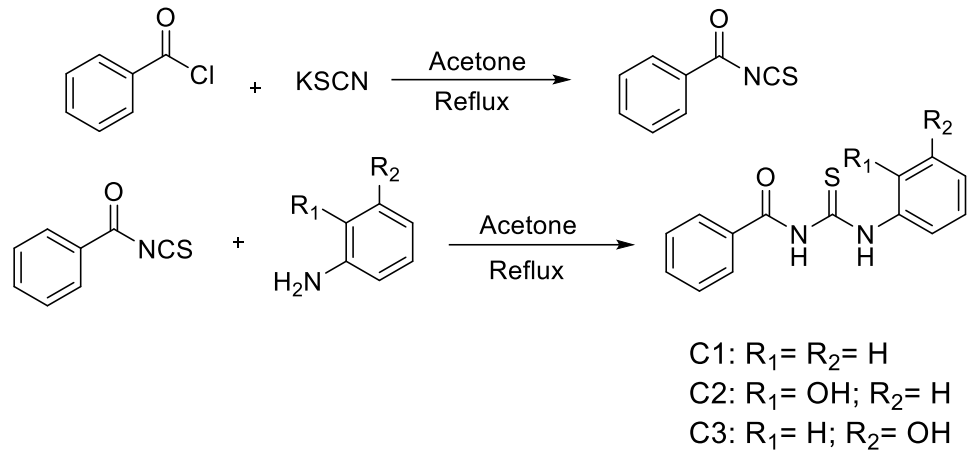

Scheme S1: Reaction scheme for the synthesis of **C1-C3**.

Synthetic Procedure:

0.1 mol of Potassium thiocyanate was dissolved in acetone. To it, 0.1 mol of the acylating agent *i.e.* Benzoyl chloride was added slowly with constant shaking. The mixture was then refluxed for 15 min, cooled and filtered. To the filtrate, 0.1 mol of amine dissolved in acetone was slowly added and the mixture was shaken. The mixture was then refluxed for 10 min and thereafter acetone was removed by distillation. In a beaker containing crushed ice, the mixture was added slowly with constant stirring and the reagent was solidified. The crude reagent was filtered and recrystallized from ethanol. **C1**, **C2** and **C3** were characterized by FT-IR, ^{1}H and ^{13}C NMR.

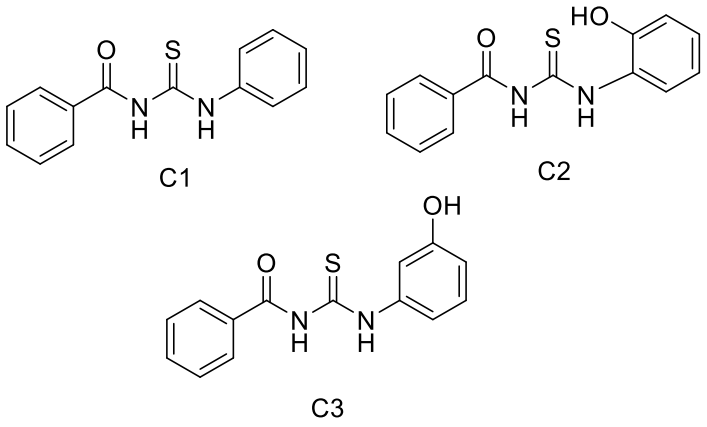

Figure S1: Structure of the receptors **C1-C3** chosen for the study.

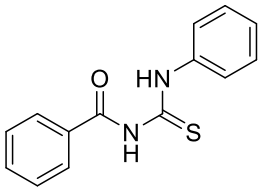

C1: White solid, Yield: 92%, FT-IR of **C1** (cm^{-1}): υ(C=O) = 1659 and υ(C=S) = 1533. ^{1}H NMR of **C1** (400 MHz, $CDCl_3$): δ_H 12.58 (s, 1H, NH), 11.53 (s, 1H, NH), 7.89 (d, 2H), 7.71 (d, 2H), 7.65 (t, 1H), 7.54 (t, 2H), 7.42 (t, 2H), 7.28 (t, 1H); ^{13}C NMR (100 MHz, $CDCl_3$) δ 178.4, 167, 137.7, 133.8, 131.7, 129.3, 129, 127.5, 127, 124.2; HRMS m/z calculated for $C_{14}H_{12}N_2OS$ $[M + H]^+$ 257.0670, found 257.0929.

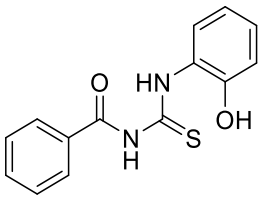

C2: Orange solid, Yield: 73%, FT-IR of **C2** (cm^{-1}): υ(C=O) = 1672 and υ(C=S) = 1527. ^{1}H NMR of **C2** (400 MHz, DMSO-d_6): δ_H (ppm) 12.93 (s, 1H, NH), 11.45 (s, 1H, NH), 10.20 (s, 1H, OH), 8.51 (d, 1H), 7.94 (d, 2H), 7.63 (t, 1H), 7.50 (t, 2H), 7.04 (t, 1H), 6.92 (d, 1H), 6.81 (t, 1H); ^{13}C NMR (100 MHz, DMSO-d_6) δ 178,168.8, 149.4, 133.6, 132.7, 129.2, 128.9, 127, 126.4, 123.7, 118.8, 115.6; HRMS m/z calculated for $C_{14}H_{12}N_2O_2S$ $[M + H]^+$ 273.0619, found 273.0697.

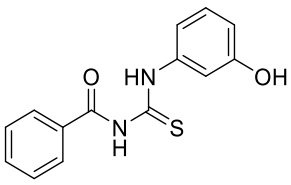

C3: Off white solid, Yield: 41%, FT-IR of **C3** (cm^{-1}): υ(C=O) = 1674, υ(C=S) = 1536. ^{1}H-NMR of **C3** (400 MHz, DMSO-d_6): δ_H 12.55 (s, 1H, NH), 11.48 (s, 1H, NH), 9.60 (s, 1H, OH), 7.94 (d, 2H), 7.62 (t, 1H), 7.50 (t, 2H), 7.25 (s, 1H), 7.17 (t, 1H), 7.02 (d, 1H), 6.64 (d, 1H); ^{13}C NMR (100 MHz, DMSO-d_6) δ 179.1, 168.8, 158, 139.4, 133.6, 132.6, 130, 129.2, 128.9, 115, 113.9, 111.4; HRMS m/z calculated for $C_{14}H_{12}N_2O_2S$ $[M + H]^+$ 273.0619, found 273.0694.

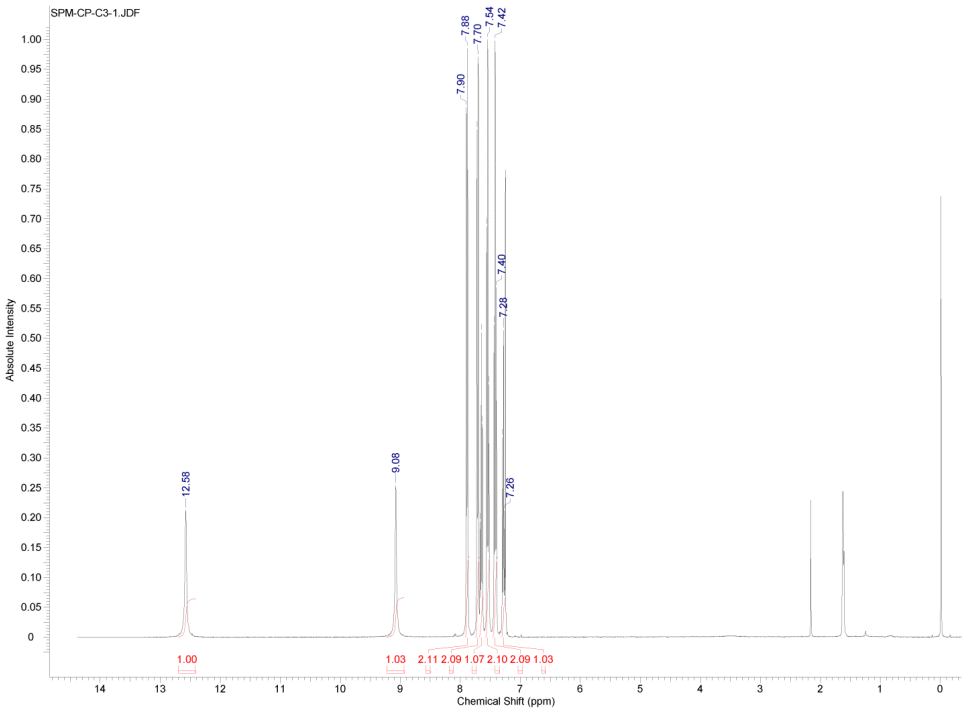

Figure S2: ^{1}H NMR spectrum of **C1** ($CDCl_3$, 298 K)

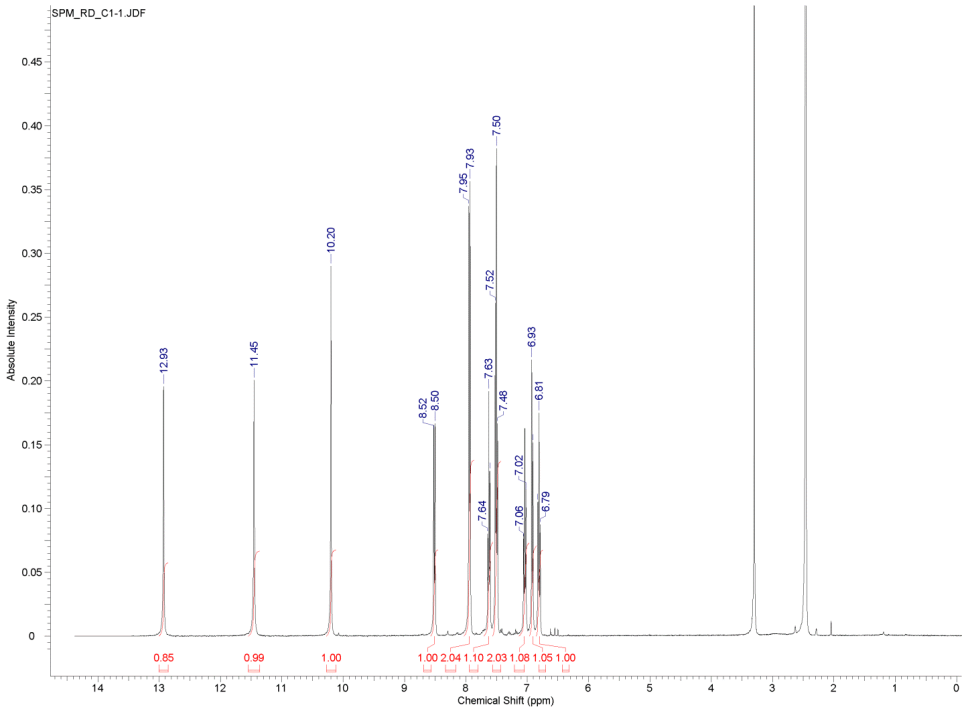

Figure S3: ^{1}H NMR spectrum of **C2** (DMSO-d_6, 298 K).

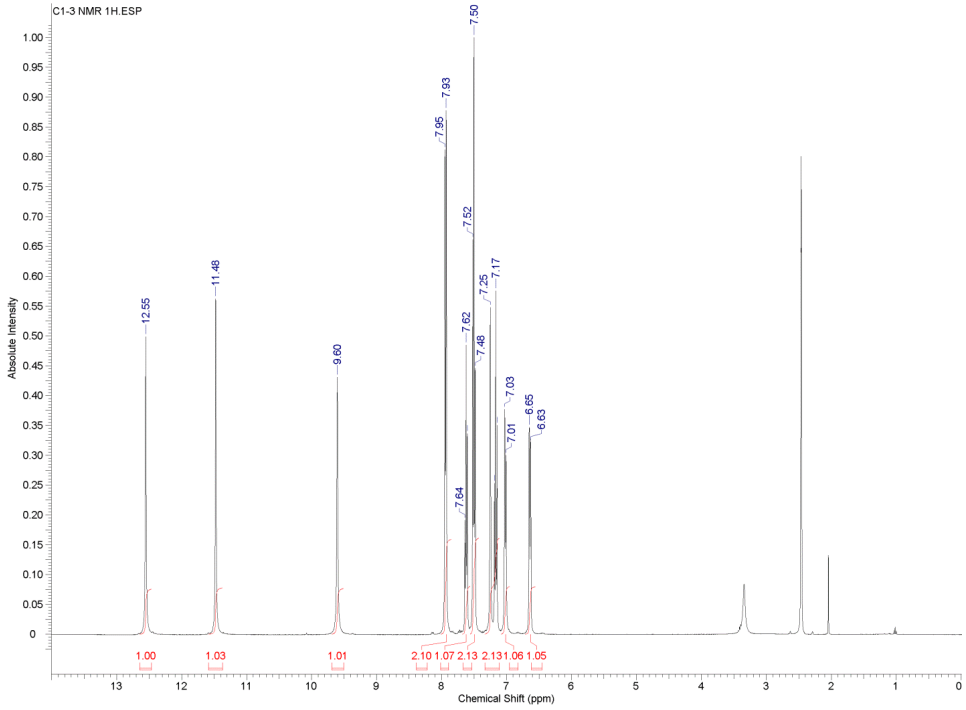

Figure S4: ^{1}H NMR spectrum of **C3** (DMSO-d_6, 298 K).

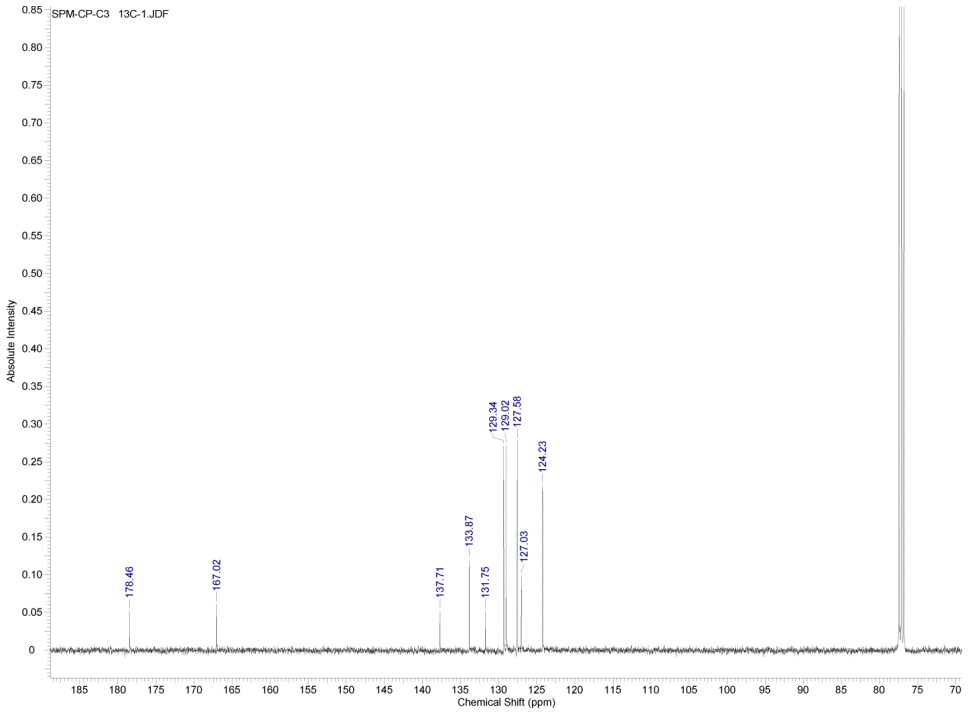

Figure S5: ^{13}C NMR spectrum of **C1** ($CDCl_3$, 298 K)

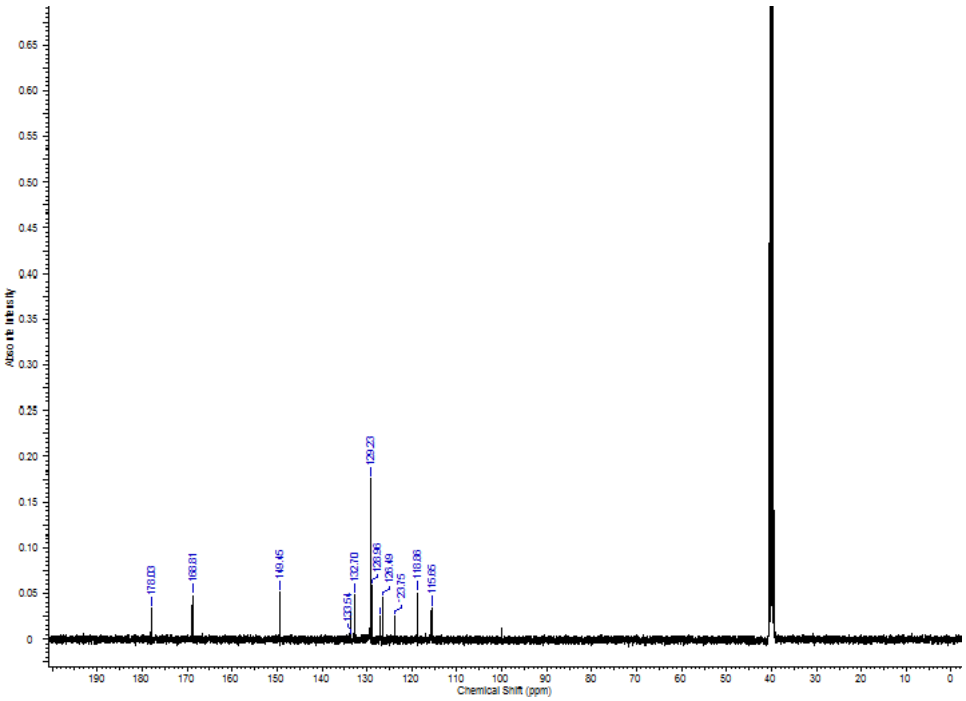

Figure S6: ^{13}C NMR spectrum of **C2** (DMSO-d_6, 298 K).

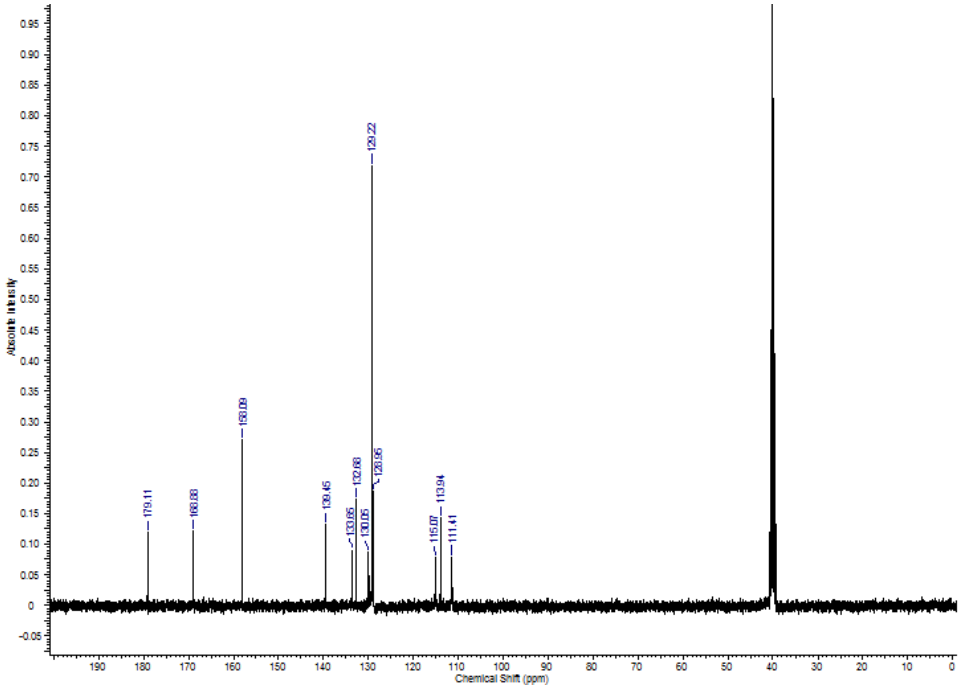

Figure S7: ^{13}C NMR spectrum of **C3** (DMSO-d_6, 298 K).

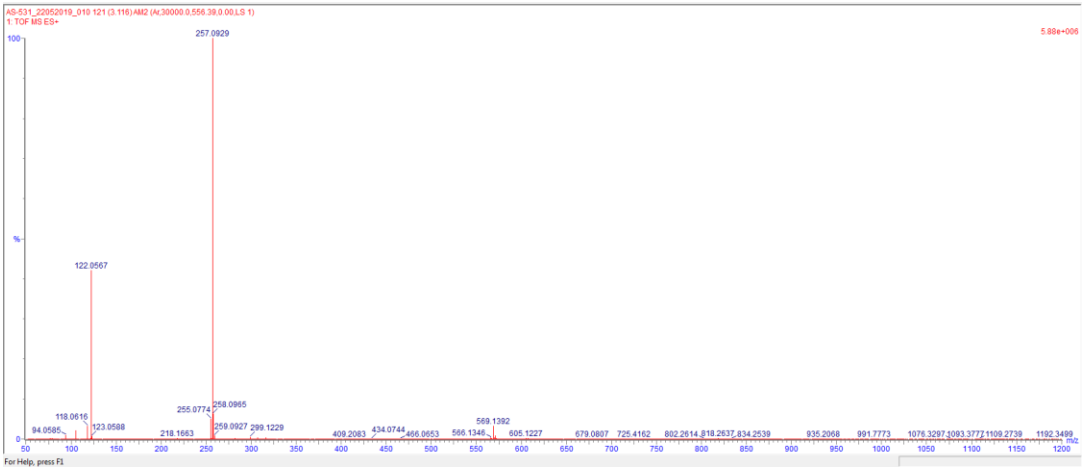

Figure S8: HRMS of **C1**

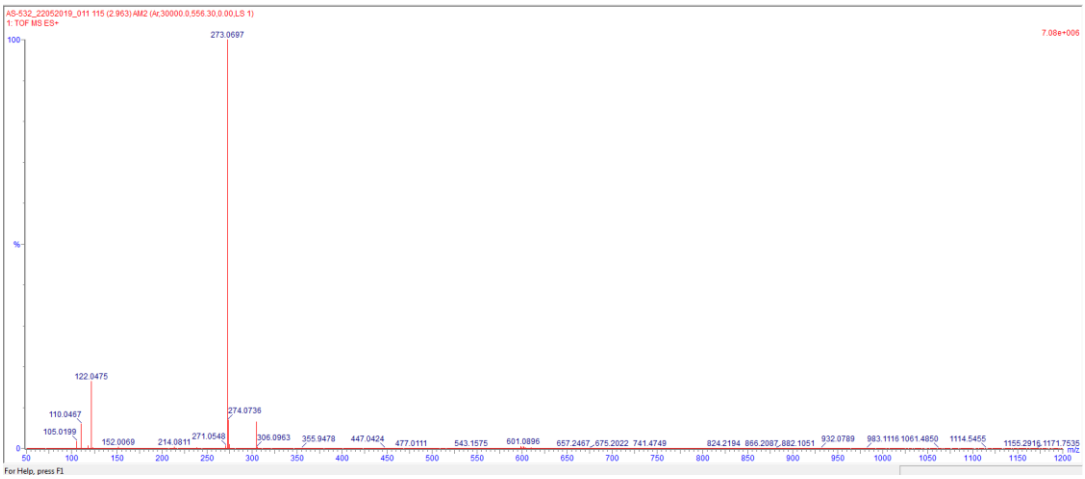

Figure S9: HRMS of **C2**

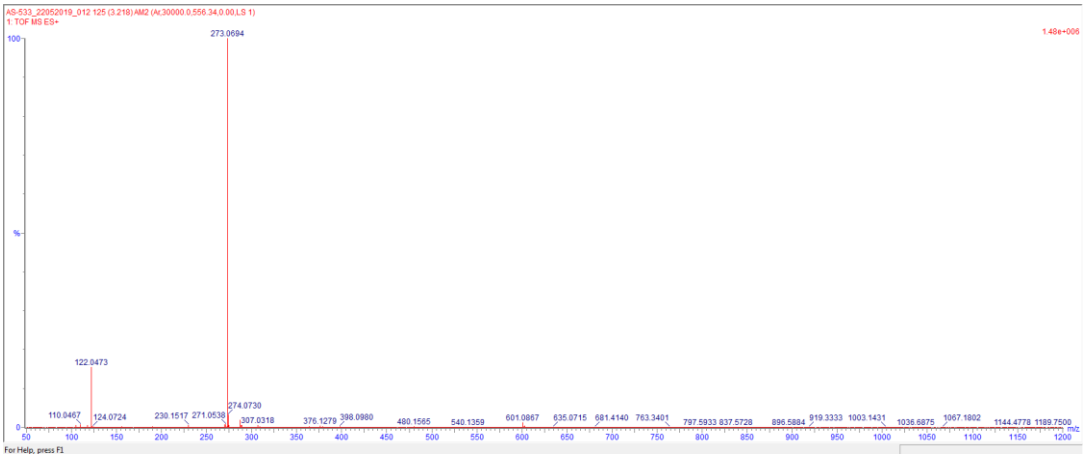

Figure S10: HRMS of **C3**

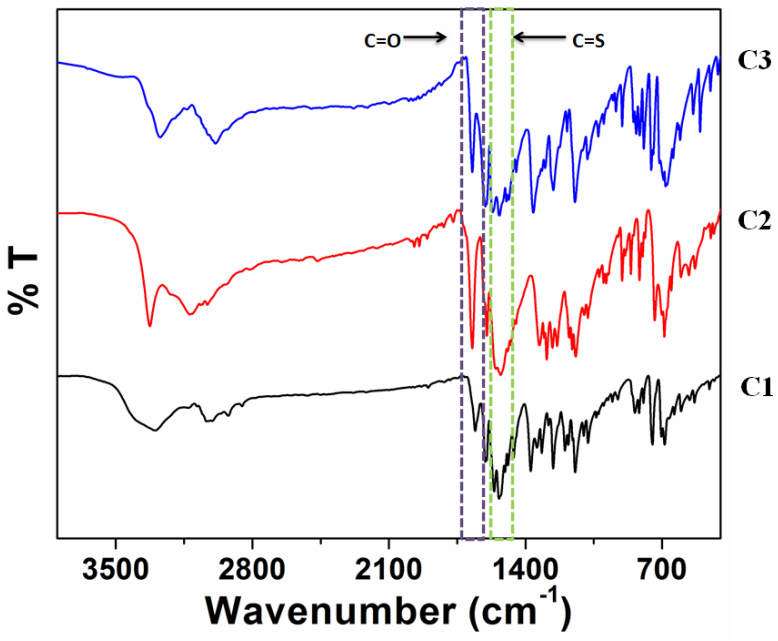

Figure S11: Stack plot of FT IR spectra for **C1**-**C3**. *IR spectra measured as KBr discs

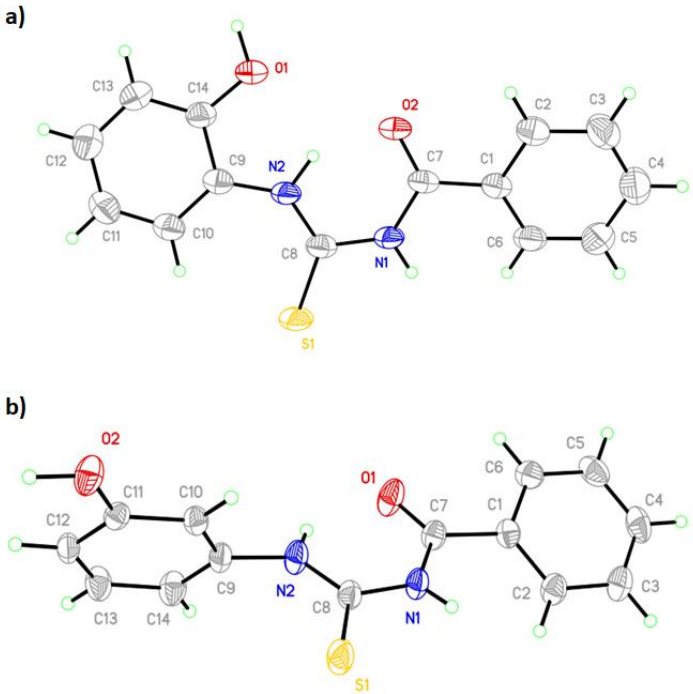

Figure S12: a) ORTEP diagram of **C2** with 50% probability ellipsoid; b) ORTEP diagram of **C3** with 50% probability ellipsoid

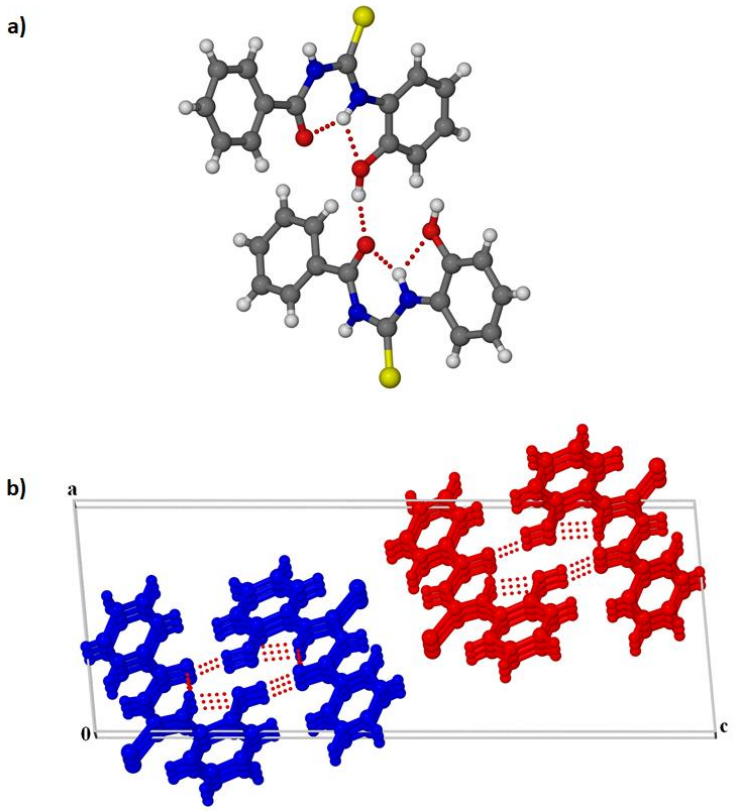

Figure S13: Packing diagram of **C2** viewed along b axis. The dashed lines indicate hydrogen bonds.

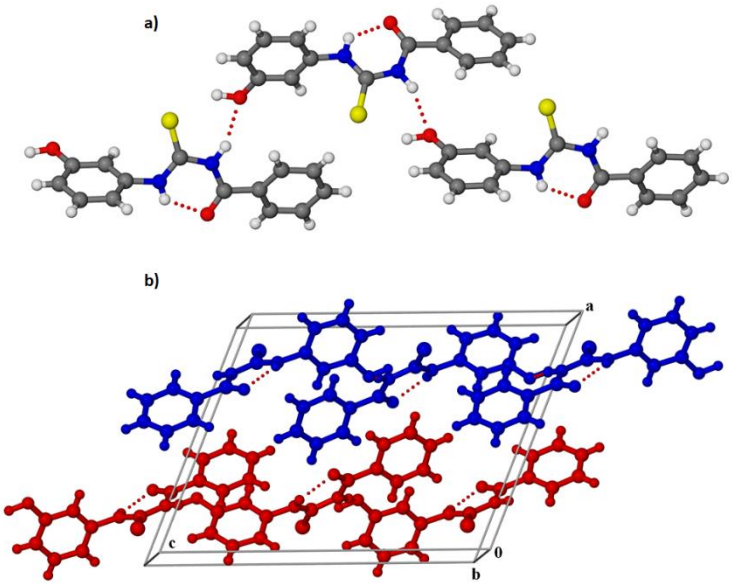

Figure S14: Packing diagram of **C3** viewed along b axis. The dashed lines indicate hydrogen bonds.

Compound	C2	C3
CCDC number	2065030	2065031
Empirical formula	$C_{14}H_{12}N_2O_2S$	$C_{14}H_{12}N_2O_2S$
Formula weight (g/mol)	272.32	272.32
Temperature/K	296	296
Crystal system	Monoclinic	Monoclinic
Space group	*P* 2_1/n	*P* 2_1/c
a/Å	9.7375(17)	12.2027(10)
b/Å	5.1423(9)	7.3419(6)
c/Å	25.972(5)	15.7431(13)
α/°	90.00	90.00
β/°	95.230(5)	112.224(2)
γ/°	90.00	90.00
Volume/$Å^3$	1295.1(4)	1305.66(19)
Z	4	4
Density, $\rho_{calc}g/cm^3$	1.397	1.385
Absorption coefficient, μ/mm^{-1}	0.249	0.247
F(000)	568	568
Crystal size/mm^3	0.250 x 0.090 x 0.070	0.260 x 0.150 x 0.120
Radiation	MoKα (λ = 0.71073 Å)	MoKα (λ = 0.71073 Å)
2Θ range for data collection/°	4.040 to 25.025	1.803 to 25.022
Index ranges	$-10 \le h \le 11$, $-6 \le k \le 6$, $-30 \le l \le 30$	$-14 \le h \le 14$, $-8 \le k \le 8$, $-18 \le l \le 18$
Reflns. Collected	20726	17381
Unique Reflns.	2257	2284
Observed Reflns.	1579	2014
Data/restraints/parameters	2257/1/184	2284/1/184
Goodness-of-fit on F^2	1.025	1.047
Final R indexes [I>=2σ (I)]	R = 0.0418; wR = 0.1036	R = 0.0344; wR = 0.0939
Final R indexes [all data]	R = 0.0659; wR = 0.1192	R = 0.0395; wR = 0.0983

Table S1: The crystallographic parameters for compound **C2** and **C3**.

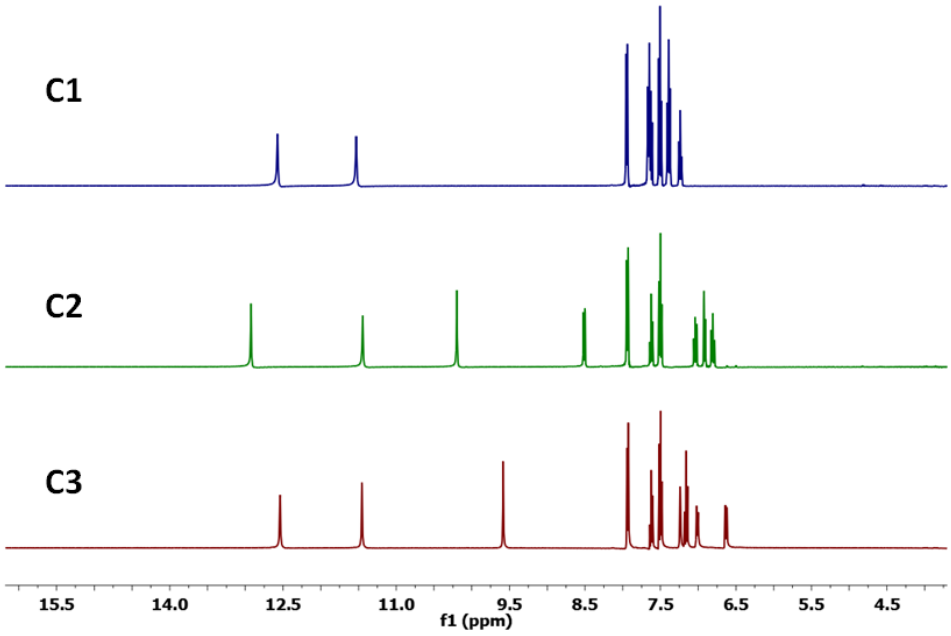

Figure S15: Stack plot for **C1-C3** recorded by ^{1}H NMR spectroscopy (DMSO-d_6, 298 K).

2D NMR analysis

For **C2:**

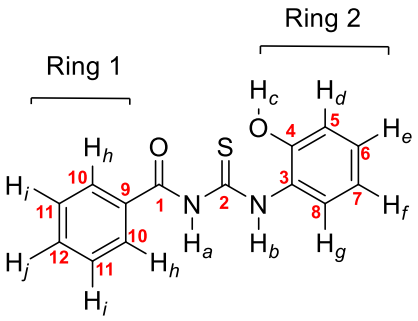

In the ^{1}H-NMR spectrum of **C2**, we observed a doublet and two triplets at δ 7.94, 7.62 and 7.50 ppm for 2H, 1H and 2H respectively. As there is no other possibility for a doublet and triplet with integration value of 2H, so the signal at δ 7.94 and 7.50 ppm must be for H_h and H_i respectively. Additionally, a correlated spectroscopy (COSY) correlation is observed between triplets at δ 7.62 and 7.50 ppm, thereby pointing the triplet at δ 7.62 ppm for H_j. Based on the correlations observed in HSQC spectrum, the signals arising at δ 128.9, 133.6 and 129.2 can be assigned to C-10, C-12 and C-11 respectively. Furthermore, the ^{13}C-NMR spectrum shows signals for C-1 and C-2 at δ 168.8 and 178 ppm respectively for

the C=O and C=S moiety. Moreover, in the HSQC spectrum we did not observe any correlations corresponding to the ^{13}C-NMR signals at δ 149.4, 132.7 and 126.5 ppm, which gave us the impression that these signals might be either for C-4, C-9 or C-3 atom. The HMBC confirmed the signal at δ 132.7 ppm to be for the C-9 atom as it showed a correlation with the signal for H_i protons. In the aromatic region, C-4 being the highly deshielded carbon atom on being attached to the hydroxyl group can be assigned to signal appearing at δ 149.4, which does not show any correlation in HSQC spectrum but shows very good correlations with proton signal appearing at δ 8.51 ppm in HMBC. Similarly, the C-3 carbon atom can be assigned to the signal appearing at δ 126.6 ppm, which is further confirmed by the correlation observed in HMBC with the proton signal appearing at δ 6.32 ppm. Thus, the proton signal at δ 8.51 and 6.92 ppm can be assigned to H_g and H_d proton respectively. Likewise, the proton signal at δ 7.04 and 6.81 ppm show good HMBC correlation with C-4 and C-3 carbon atoms respectively, helping us to assign them for H_e and H_f protons.

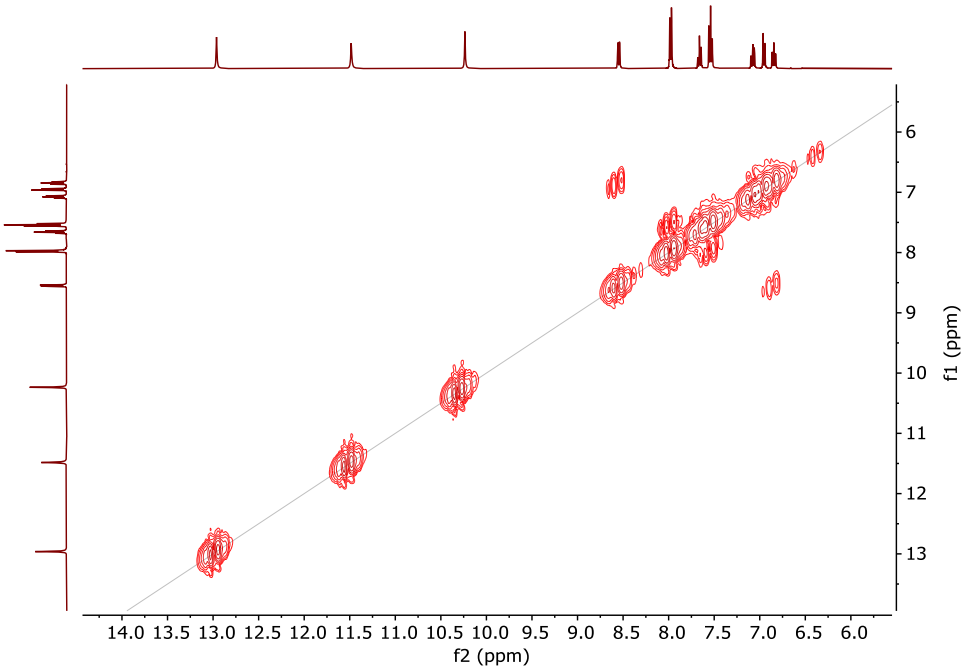

Figure S16: ^{1}H-^{1}H COSY-NMR (600 MHz) spectrum of complex **C2** in DMSO-d_6.

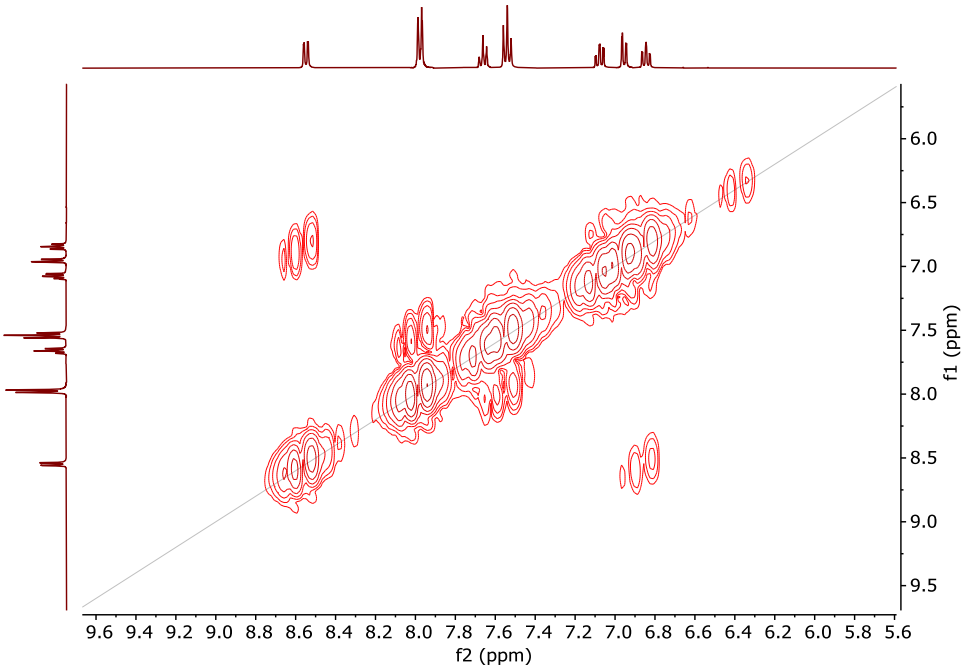

Figure S17: Expanded ^{1}H-^{1}H COSY-NMR (600 MHz) spectrum of complex **C2** in DMSO-d_6.

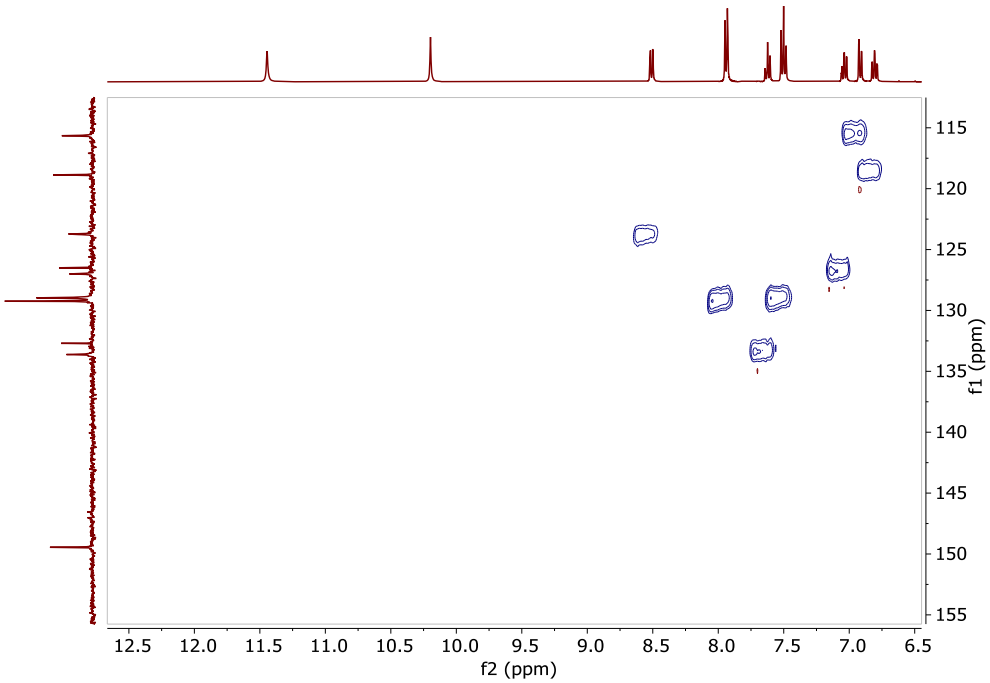

Figure S18: Expanded HSQC spectrum (600 MHz) of **C2** in DMSO-d_6.

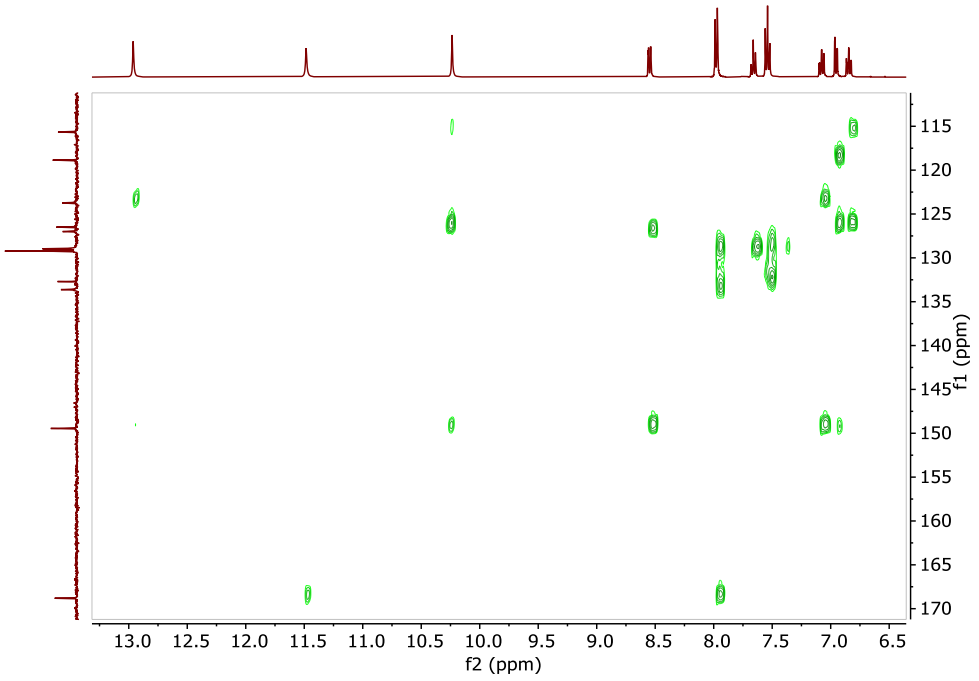

Figure S19: ^{1}H-^{13}C HMBC-NMR (600 MHz) spectrum of complex **C2** in DMSO-d_6.

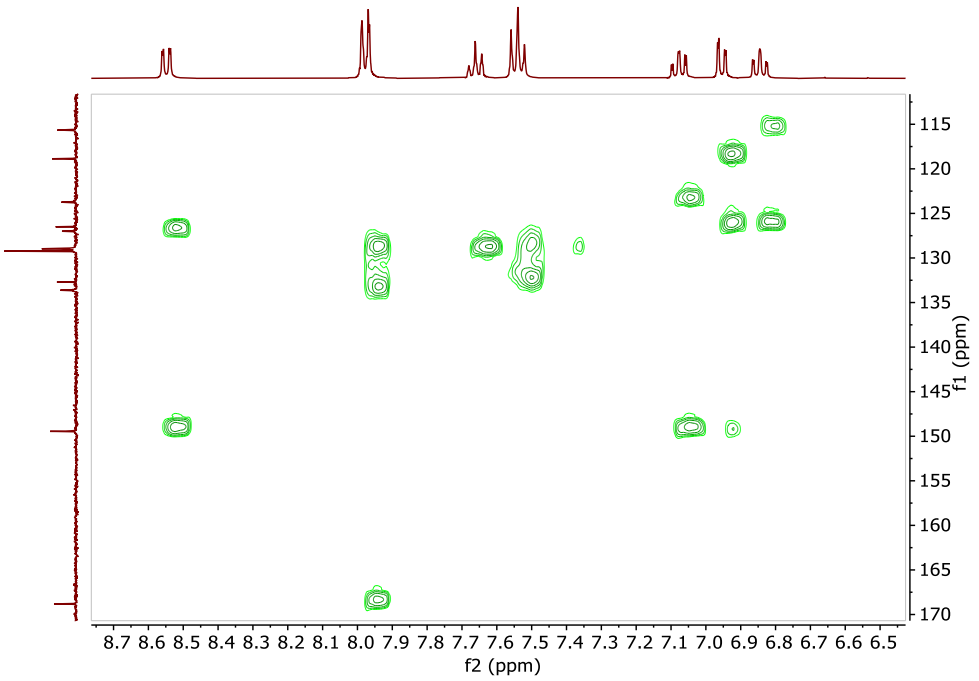

Figure S20: Expanded ^{1}H-^{13}C HMBC-NMR (600 MHz) spectrum of complex **C2** in DMSO-d_6.

Lastly in the NOESY spectrum, the proton signal at δ 11.45 ppm shows a correlation with the signals for H_h, pointing it to be the signal for NH_a. Similarly, the proton signal at δ 10.20 ppm shows a NOESY correlation with signals assigned for H_d protons, confirming the signal for OH_c. Naturally, the signal proton signal at δ 12.92 ppm is assigned to NH_b proton.

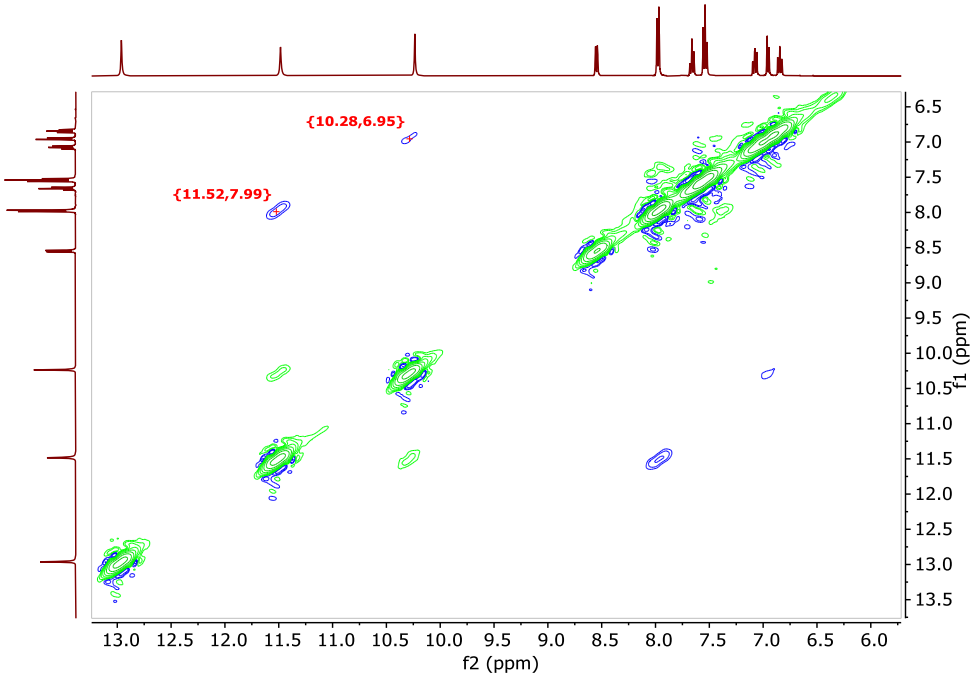

Figure S21: ^{1}H-^{1}H NOESY-NMR (600 MHz) spectrum of complex **C2** in DMSO-d_6

For **C3:**

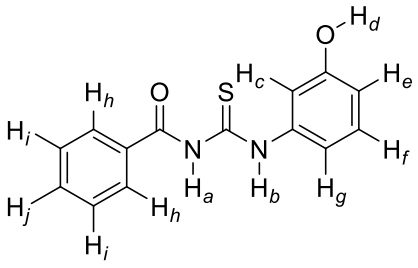

The ^{1}H-NMR spectrum of **C3** shows a doublet and two triplets at δ 7.98, 7.67 and 7.54 ppm for 2H, 1H and 2H respectively. As there is no other possibility for a doublet and triplet with integration value of 2H, so the signal at δ 7.98 and 7.54 ppm must be for H_h and H_i respectively. Additionally, a correlated spectroscopy (COSY) correlation is observed between triplets at δ 7.67 and 7.54 ppm, thereby pointing the triplet at δ 7.67 ppm for H_j. A singlet at δ 7.29 ppm for 1H unambiguously corresponds to H_c as the signals for other possible singlets

(NH_a, NH_b and -OH_c) are much more deshielded and appear downfield. Similarly, the triplet at δ 7.21 ppm for 1H can be attributed to signal for H_f.

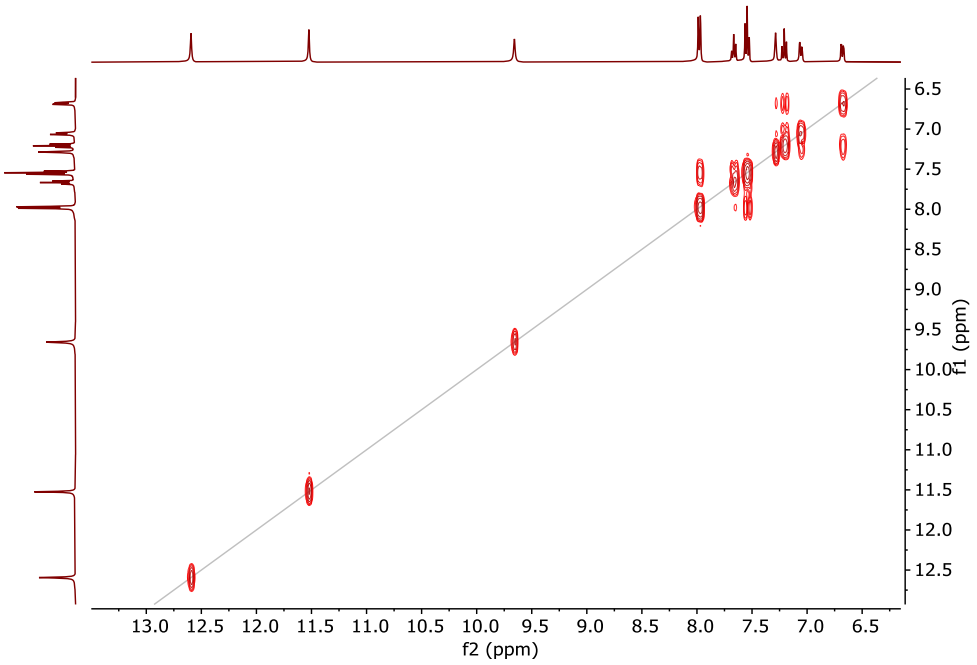

Figure S22: ^{1}H-^{1}H COSY-NMR (400 MHz) spectrum of complex **C3** in DMSO-d_6.

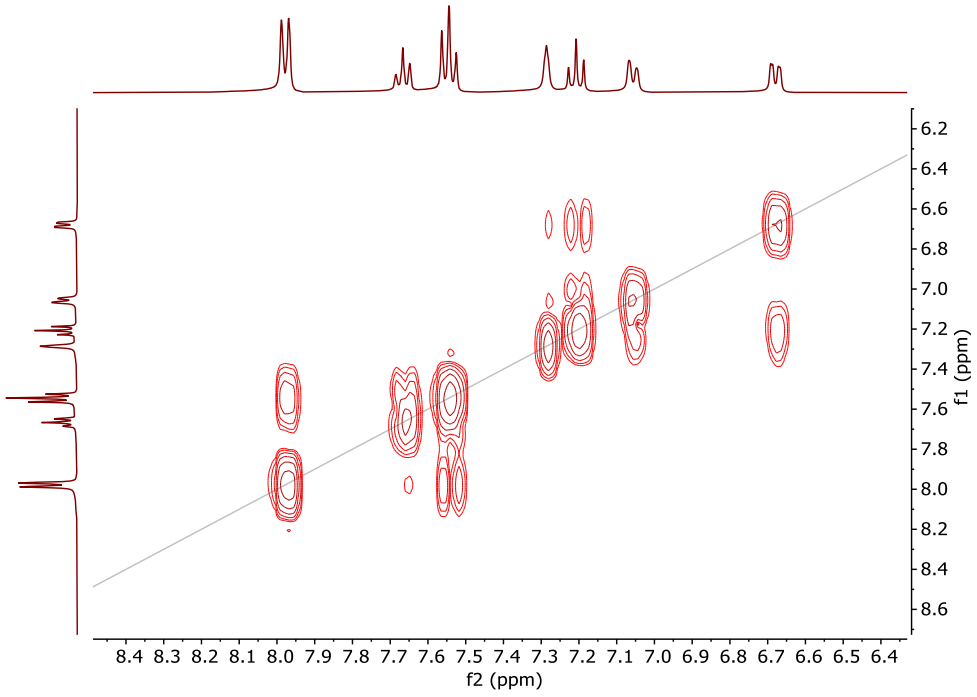

Figure S23: Expanded ^{1}H-^{1}H COSY-NMR (400 MHz) spectrum of complex **C3** in DMSO-d_6.

In the NOESY spectrum, the signal at δ 11.52 ppm shows a correlation with H_h protons, pointing it to be the signal for NH_a. Similarly, the signal at δ 12.59 ppm shows NOESY correlation with signal for NH_a and H_c, confirming the signal for NH_b. The assignment of NH_a and NH_b settles the signal at δ 9.66 ppm to OH_c proton. At this point the signals at δ 7.05 and 6.68 ppm can be designated to the H_g and H_e protons respectively owing to the NOESY correlation of OH_c proton with the signal at δ 6.68 ppm. As the signals for NH_a and NH_b could be clearly designated from COSY and NOESY NMR experiments, so we did not proceed towards complex Hetro-nuclear correlation spectroscopy.

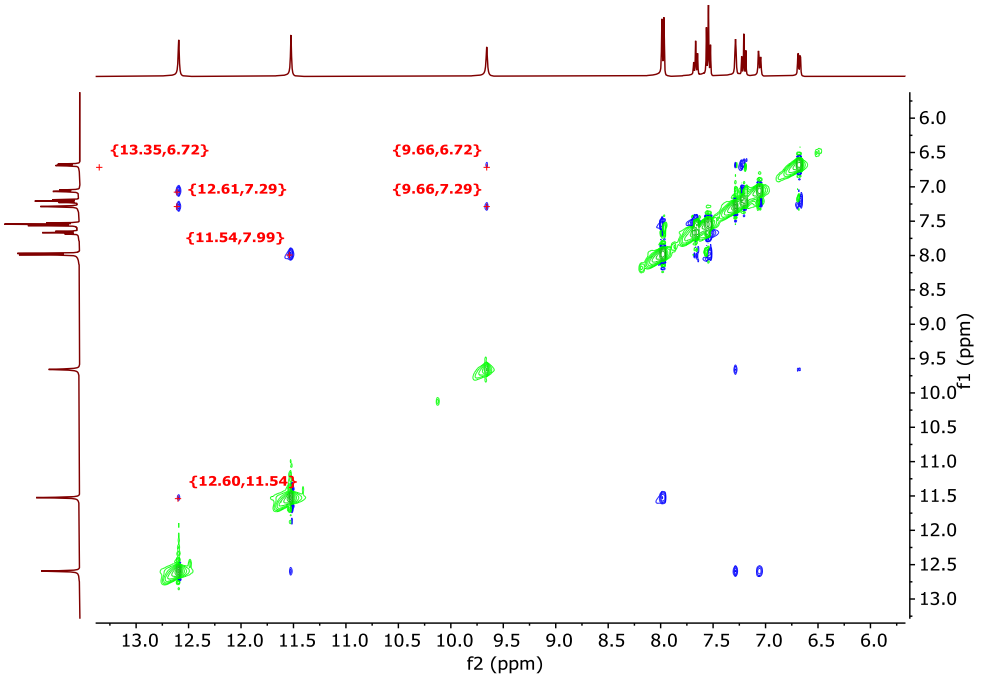

Figure S24: ^{1}H-^{1}H NOESY-NMR (600 MHz) spectrum of complex **C2** in DMSO-d_6.

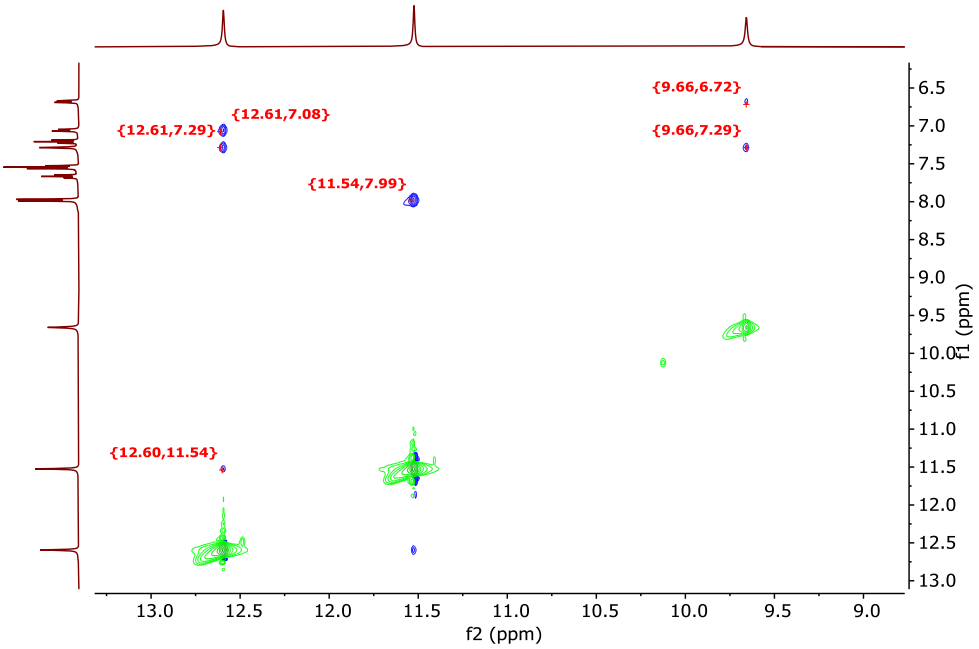

Figure S25: Expanded ^{1}H-^{1}H NOESY-NMR (600 MHz) spectrum of complex **C2** in DMSO-d_6.

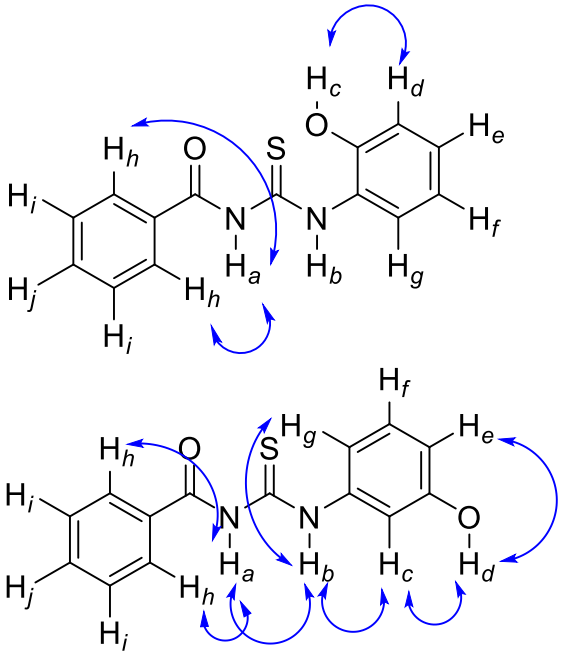

Figure S26: Important NOE interactions observed in **C2** (top) and **C3** (bottom).

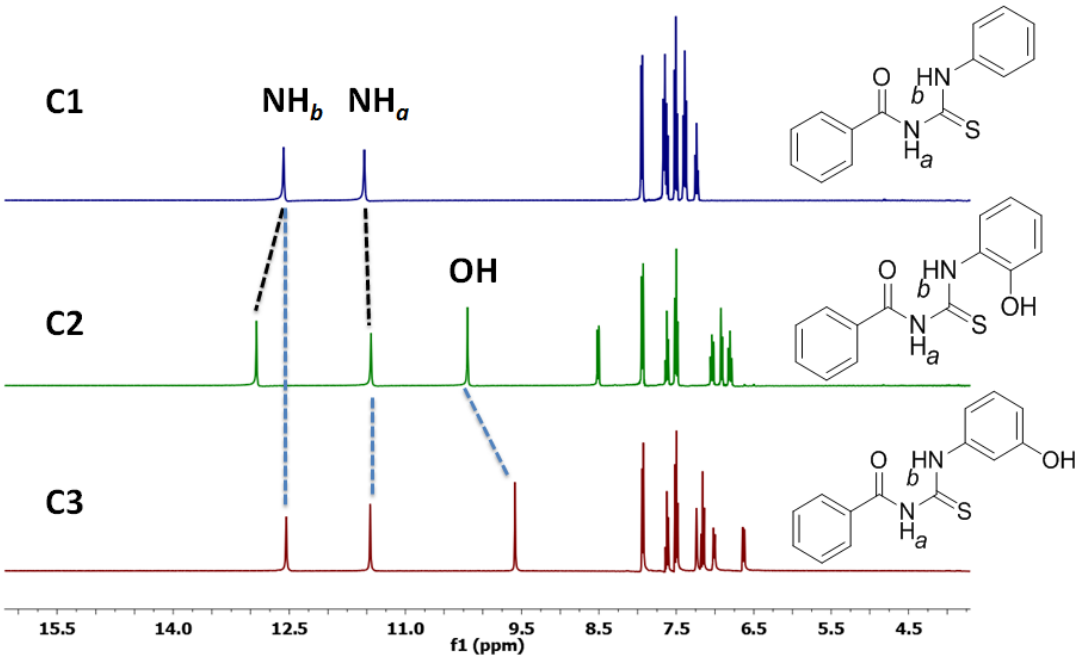

Figure S27: Stack plot for **C1**-**C3** recorded by ^{1}H NMR with designation of NH$_a$ and NH$_b$ peaks (DMSO-d_6, 298 K).

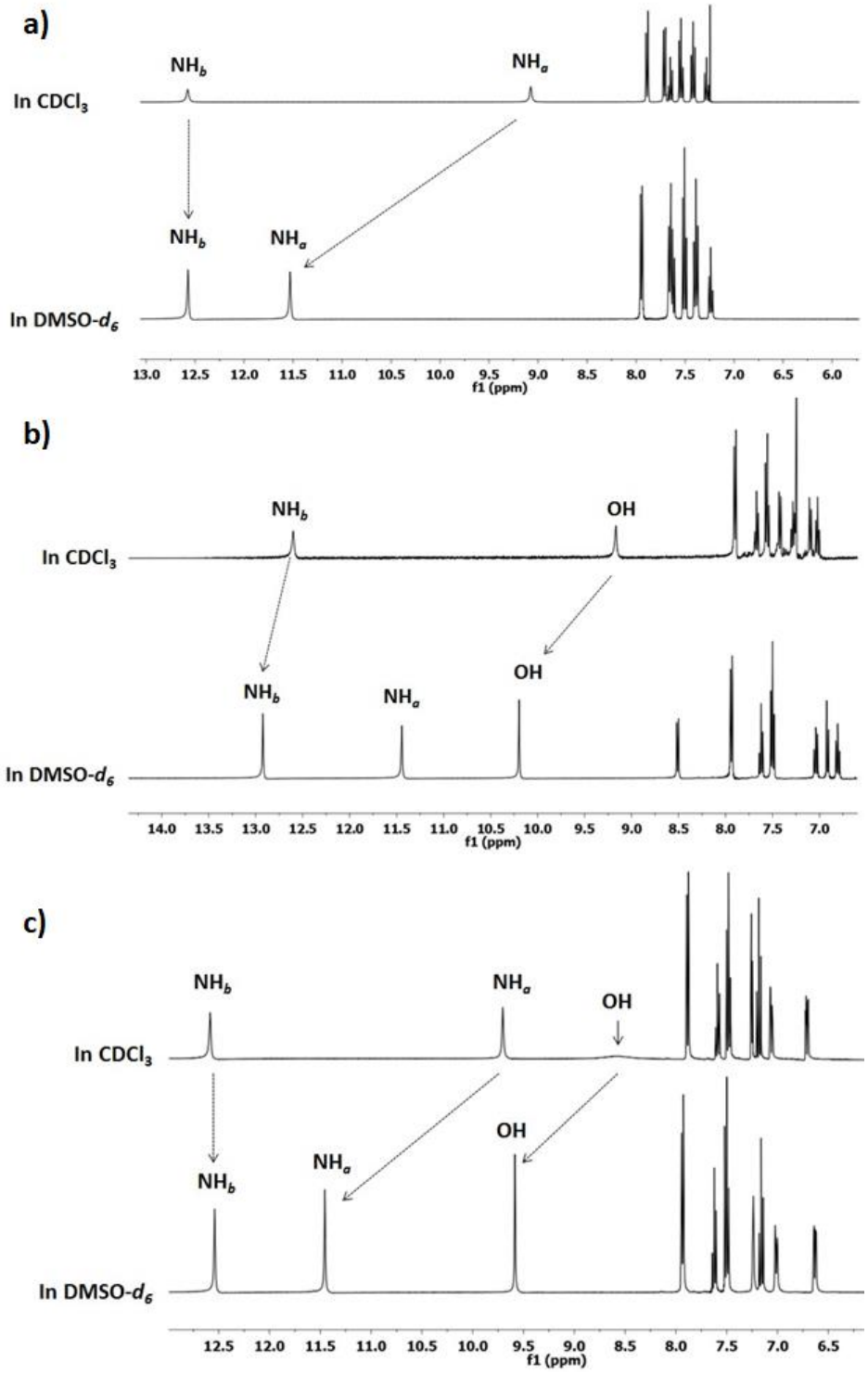

Figure S28: Changes in the ^{1}H NMR spectrum of receptor a) **C1**, b) **C2** and c) **C3** (with particular interest to the position of NH$_a$ and NH$_b$ protons) in $CDCl_3$ and DMSO-d_6.

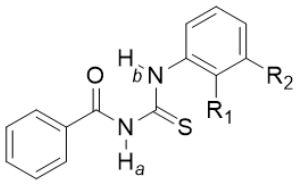

C1: $R_1 = R_2 = H$
C2: $R_1 = OH$, $R_2 = H$
C3: $R_1 = H$, $R_2 = OH$

	Chemical shift (ppm) in DMSO-d_6			Chemical shift (ppm) in $CDCl_3$		
Receptors	δNH_a	δNH_b	δOH	δNH_a	δNH_b	δOH
C1	11.53	12.57	x	9.08	12.58	x
C2	11.45	12.93	10.20	DA	12.60	9.17
C3	11.46	12.54	9.59	9.70	12.58	8.59

Figure S29: Chemical shift of the NH_a, NH_b and OH resonances for **C1**-**C3** in DMSO-d_6 and $CDCl_3$. (DA: Do not Appear)

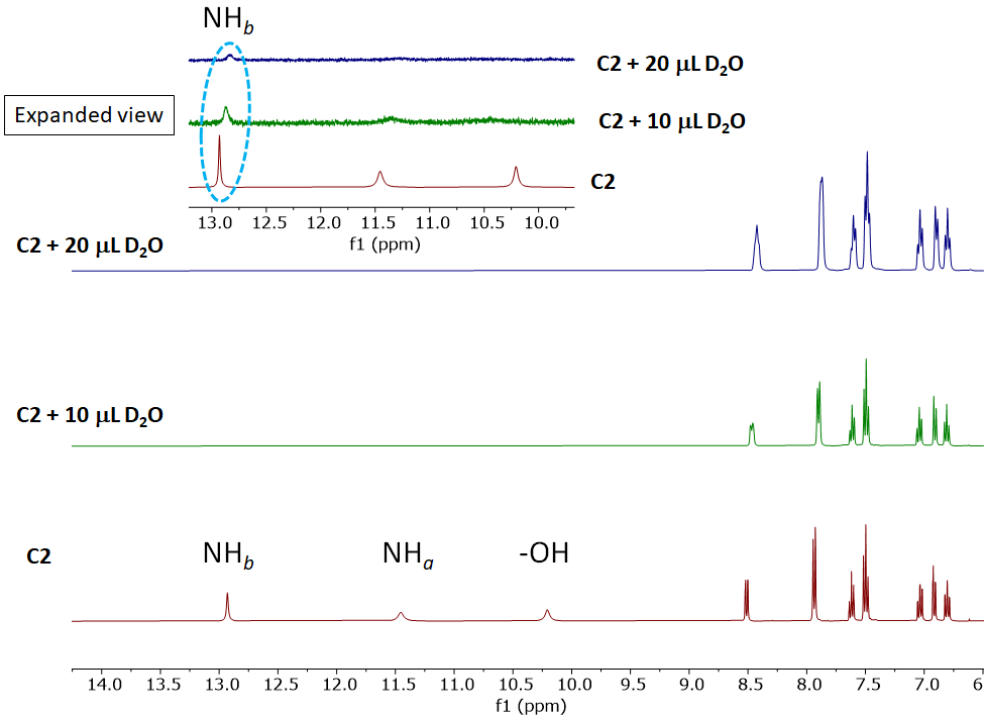

Figure S30: Changes in the ^1H NMR spectrum of receptor **C2** in DMSO-d_6 upon sequential addition of D_2O (absolute intensity).

UV-Vis study of the receptors **C1-C3**

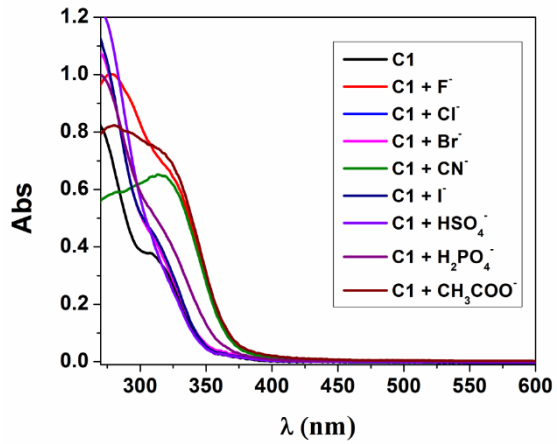

Figure S31: UV-Vis spectra for **C1** ([**C1**] = 4.7 x 10^{-5} M) in presence of different anion (50 x 10^{-3} M) as their tetraalkylammonium salt in DMSO as the solvent.

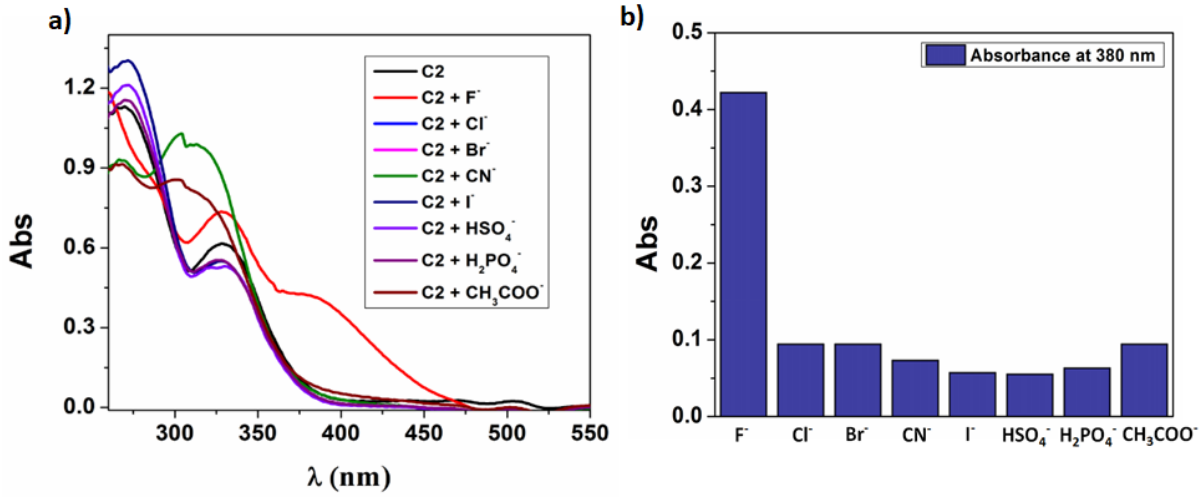

Figure S32: a) UV-Vis spectra for **C2** ([**C2**] = 6.2 x 10^{-5} M) in presence of different anions (50 x 10^{-3} M) as their tetraalkylammonium salt in DMSO as the solvent; b) Bar diagram representing UV-Vis response of **C2** in presence of different anion at λ_{max} = 380 nm.

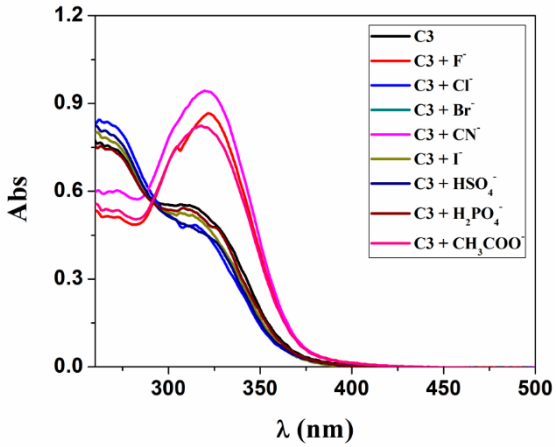

Figure S33: UV-Vis spectra for **C3** ([**C3**] = 4.7 x 10^{-5} M) in presence of different anion (50 x 10^{-3} M) in DMSO as the solvent.

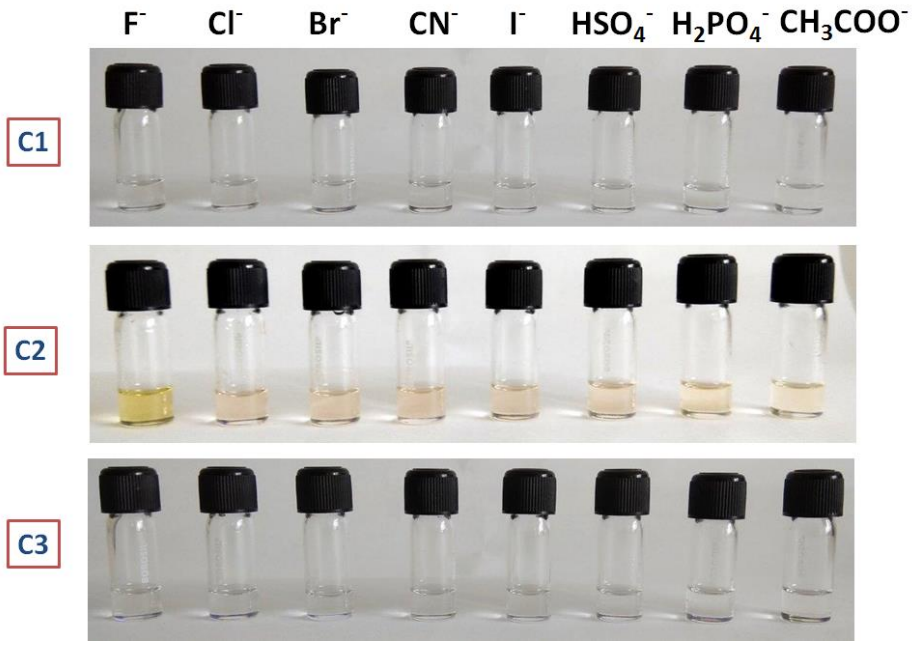

Figure S34: Image showing colorimetric response of the three receptors (**C1-C3**) in presence of different anions as their tetraalkylammonium salts in DMSO.

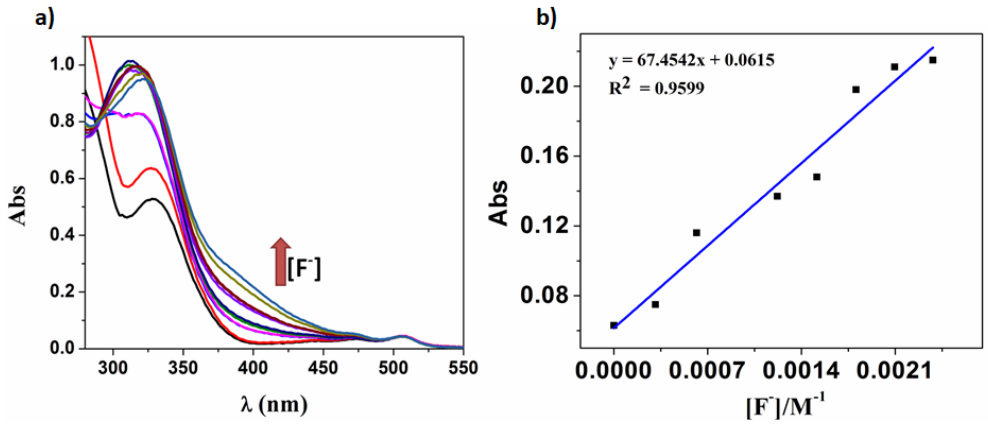

Figure S35: a) UV-Vis changes upon gradual addition of fluoride (50 x 10^{-3} M) solution in presence of **C2** ([**C2**] = 6.2 x 10^{-5} M) in DMSO; b) Calibration for the titration data of **C2** *versus* TBAF in DMSO at λ_{max} = 380nm.

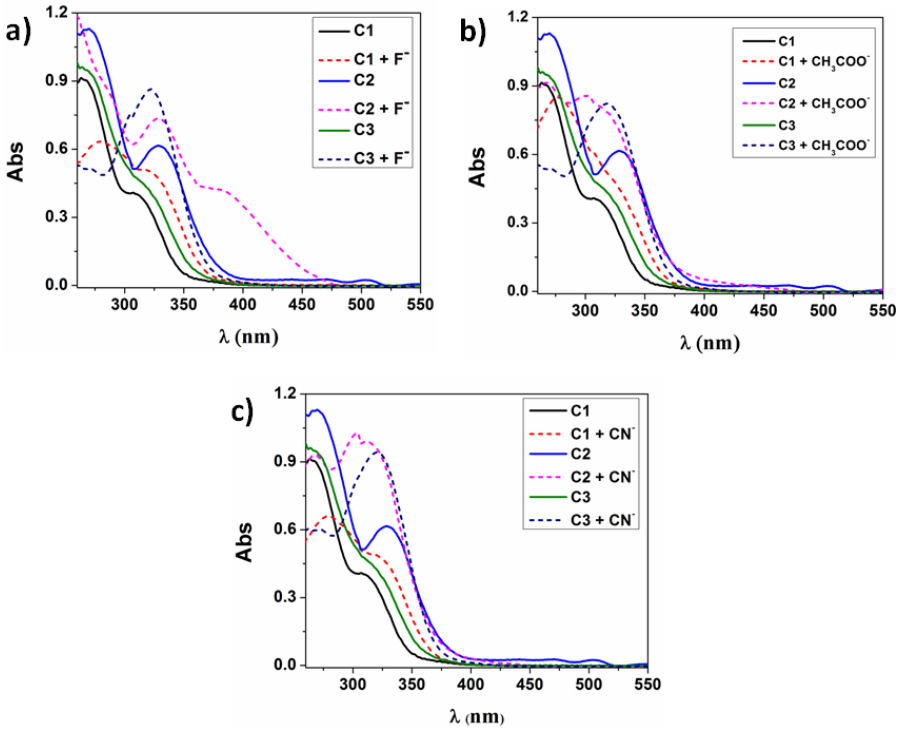

Figure S36: Comparative study of UV-Vis spectrum for **C1-C3** (6.2 x 10^{-5} M) in presence of a) F^-, b) CH_3COO^- and c) CN^- as their tetraalkylammonium salts (50 x 10^{-3} M) in DMSO.

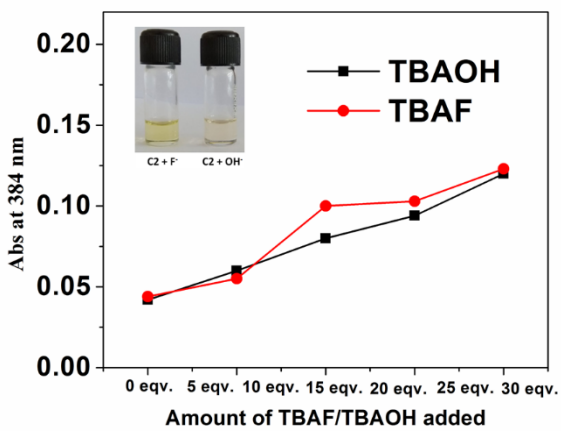

Figure S37: Comparative study of change in absorbance upon addition of different equivalents of TBAF (50 x 10^{-3} M) and TBAOH (50 x 10^{-3} M) solution to **C2** ([**C2**] = 6.2 x 10^{-5} M) w.r.t absorbance at λ = 380 nm in DMSO.

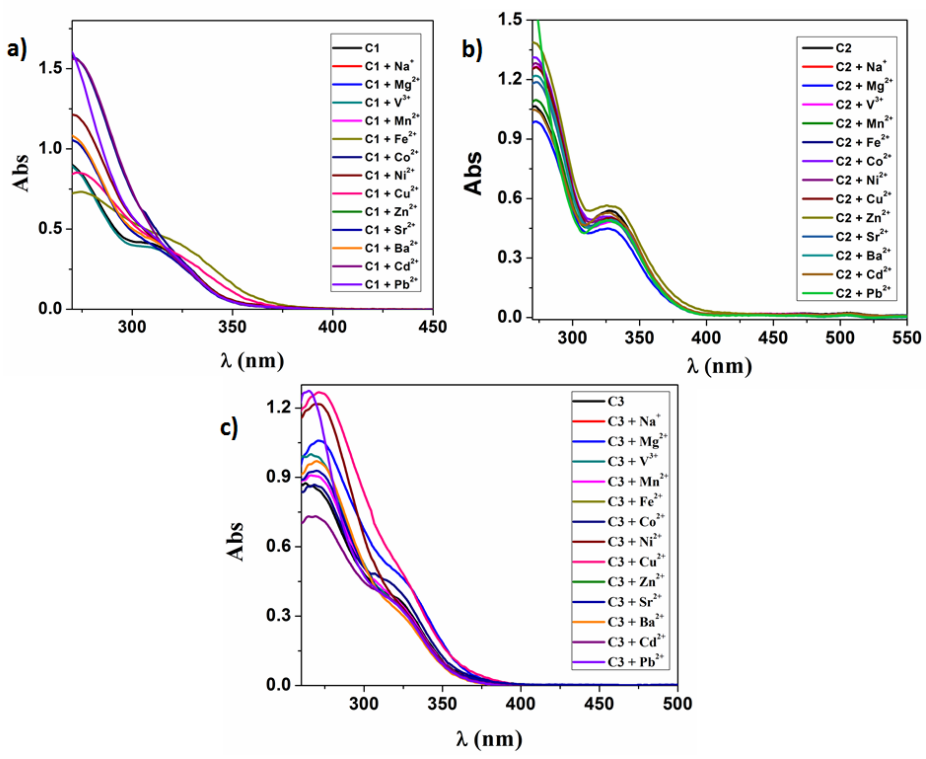

Figure S38: Change in the UV-Vis spectra of **C1-C3** (6.2 x 10^{-5} M) (a-c) in DMSO solution upon addition of different metal salts (3.8 x 10^{-4} M) (NaCl, $MgSO_4$, VCl_3, $MnCl_2$, $FeSO_4$, $CoCl_2$, $NiCl_2.6H_2O$, $CuCl_2.2H_2O$, $ZnCl_2$, $SrCl_2$, $BaSO_4$, $CdCl_2$, $PbSO_4$) as aqueous solution.

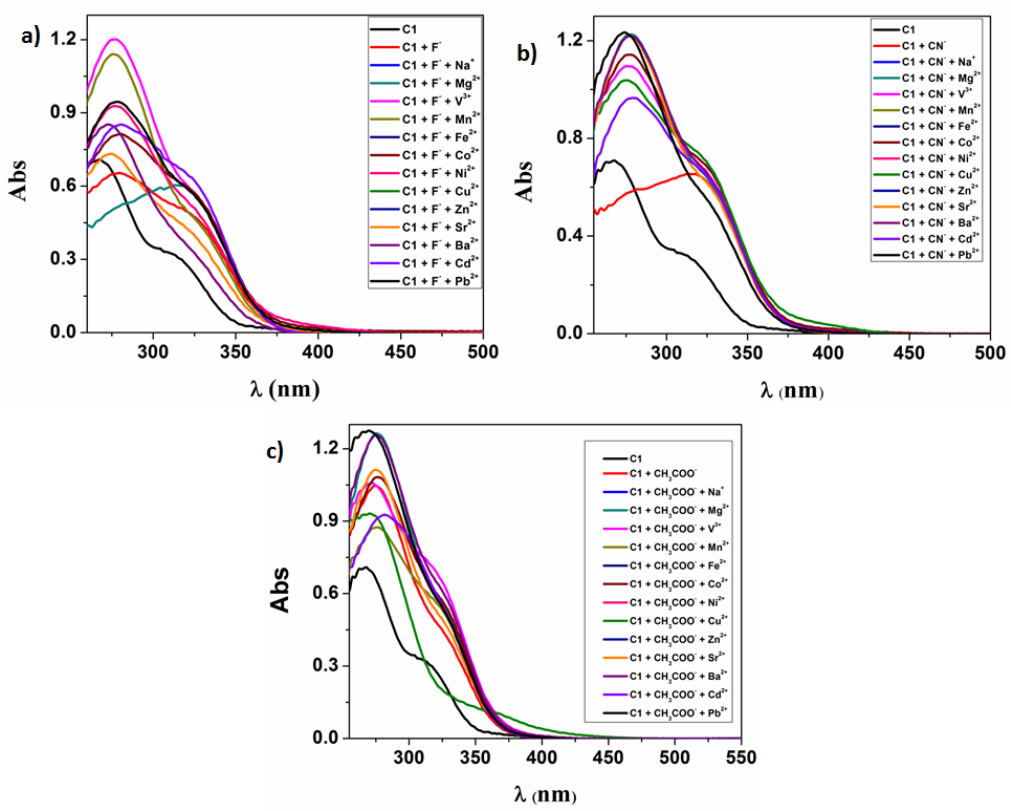

Figure S39: Change in the UV-Vis spectra of **C1**.A^- ([**C1**] = 4.7x 10^{-5} M and A = F^-, CN^-, CH_3COO^-; [F^-] = 7.8 x 10^{-4} M, [CN^-] = 7.8 x 10^{-4} M, [CH_3COO^-] = 7.8 x 10^{-4} M) in DMSO solution upon addition of different metal salts (NaCl, $MgSO_4$, VCl_3, $MnCl_2$, $FeSO_4$, $CoCl_2.6H_2O$, $NiCl_2.6H_2O$, $CuCl_2.2H_2O$, $ZnCl_2$, $SrCl_2$, $BaCl_2$, $CdCl_2$, $PbSO_4$) as aqueous solution (3.8 x 10^{-4} M).

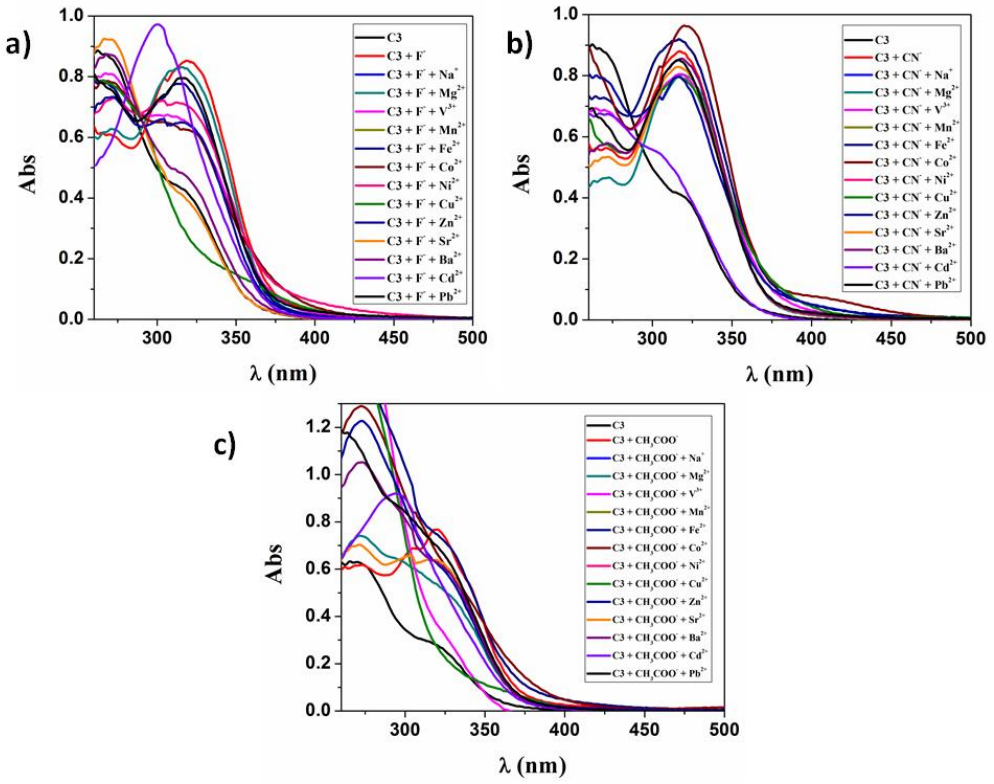

Figure S40: Change in the UV-Vis spectra of **C3**.A^- ([**C3**] = 4.7x 10^{-5} M and A = F^-, CN^-, CH_3COO^-; [F^-] = 1.5 x 10^{-3} M, [CN^-] = 1.5 x 10^{-3} M, [CH_3COO^-] = 1.5 x 10^{-3} M) in DMSO solution upon addition of different metal salts (NaCl, $MgSO_4$, VCl_3, $MnCl_2$, $FeSO_4$, $CoCl_2.6H_2O$, $NiCl_2.6H_2O$, $CuCl_2.2H_2O$, $ZnCl_2$, $SrCl_2$, $BaSO_4$, $CdCl_2$, $PbSO_4$) as aqueous solution (3.8 x 10^{-4} M).

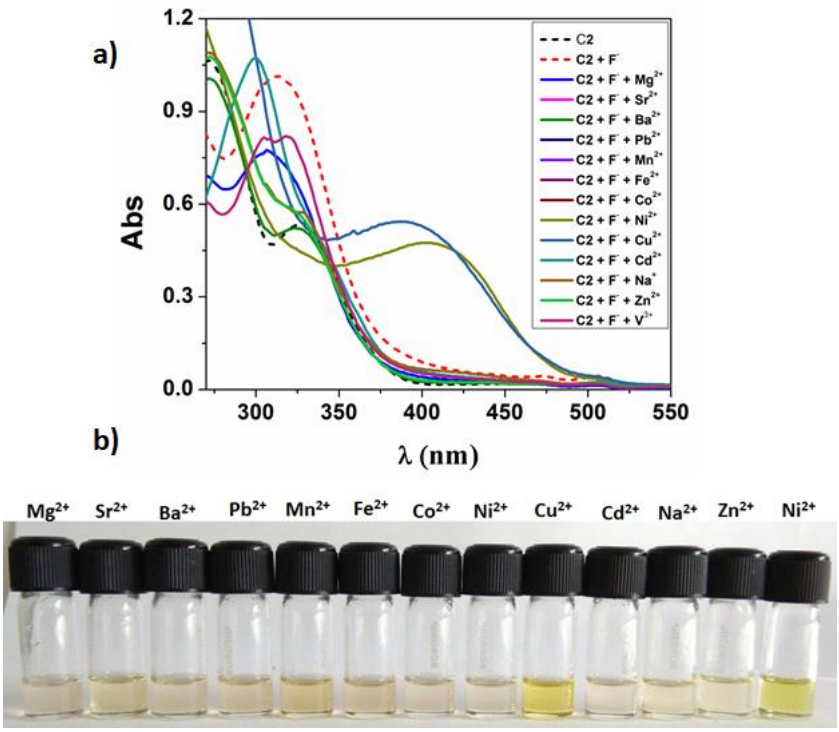

Figure S41: a) Change in the UV-Vis spectra of **C2**.F^- ([**C2**] = 6.2 x 10^{-5} M, [F^-] = 1.53 x 10^{-3} M) in DMSO solution upon addition of different metal salts (NaCl, $MgSO_4$, VCl_3, $MnCl_2$, $FeSO_4$, $CoCl_2.6H_2O$, $NiCl_2.6H_2O$, $CuCl_2.2H_2O$, $ZnCl_2$, $SrCl_2$, $BaSO_4$, $CdCl_2$, $PbSO_4$) as aqueous solution; b) Image showing colorimetric response of **C2**.F^- ([**C2**] = 6.2 x 10^{-5} M, [F^-] = 0.15 x 10^{-3} M) in presence of different metal ions (as their aqueous salt solution) in DMSO.

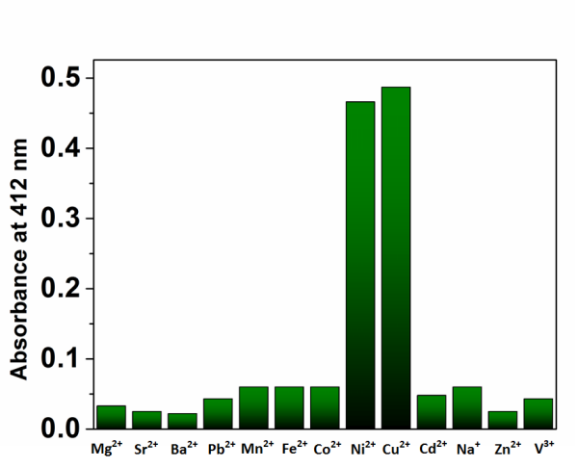

Figure S42: Bar diagram corresponding to the absorbance at 405 nm for **C2**.F^- ([**C2**] = 6.2 x 10^{-5} M, [F^-] = 1.53 x 10^{-3} M) solution in DMSO solution in presence of different metal ions screened.

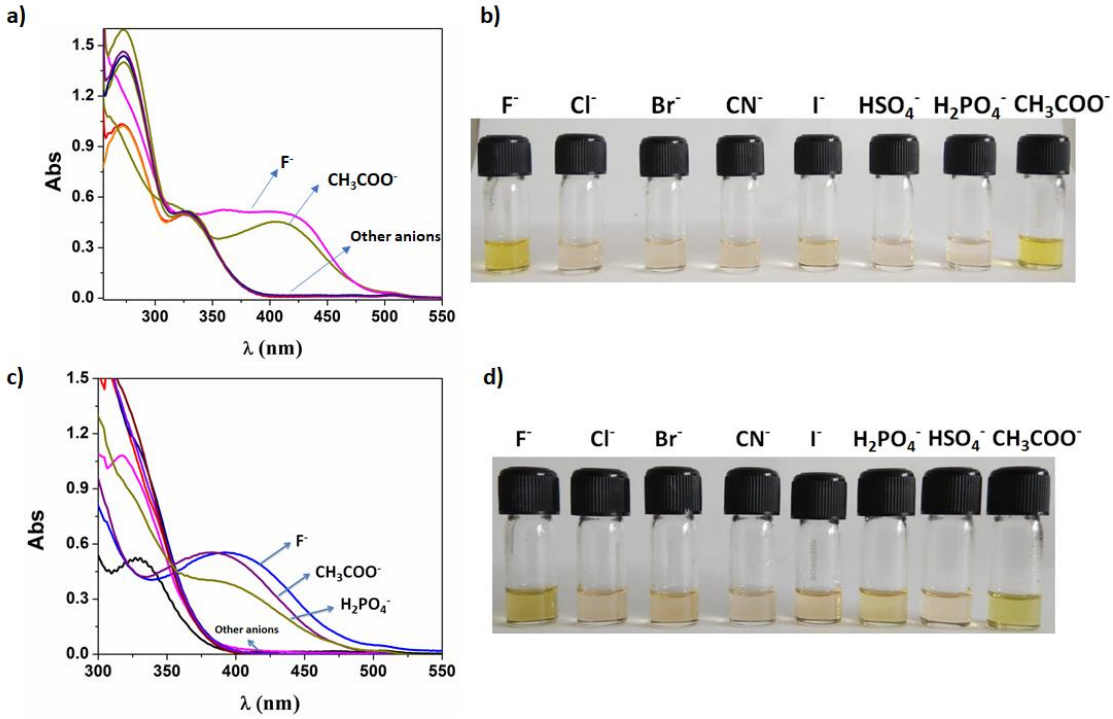

Figure S43: a) Change in the UV-Vis spectra of **C2** solution ([**C2**] = 6.2 x 10^{-5} M) in DMSO upon sequential addition of aqueous $NiCl_2.6H_2O$ ([Ni^{2+}] = 3.8 x 10^{-4} M) solution and different anions (F^-, Cl^-, Br^-, CN^-, I^-, $H_2PO_4^-$, HSO_4^-, CH_3COO^-) as their tetraalkylammonium salt (50 x 10^{-3} M) in DMSO; b) Photograph showing colorimetric change upon sequential addition of various anions as their tetraalkylammonium salt to **C2**:Ni^{2+} mixture in DMSO/water; c) Change in the UV-Vis spectra of **C2** solution ([**C2**] = 6.2 x 10^{-5} M) in DMSO upon sequential addition of aqueous $CuCl_2.2H_2O$ ([Cu^{2+}] = 3.8 x 10^{-4} M) solution and different anions (F^-, Cl^-, Br^-, CN^-, I^-, $H_2PO_4^-$, HSO_4^-, CH_3COO^-) as their tetraalkylammonium salt (50 x 10^{-3} M) in DMSO; d) Photograph showing colorimetric change upon sequential addition of various anions as their tetraalkylammonium salt to **C2**:Cu^{2+} mixture in DMSO/water.

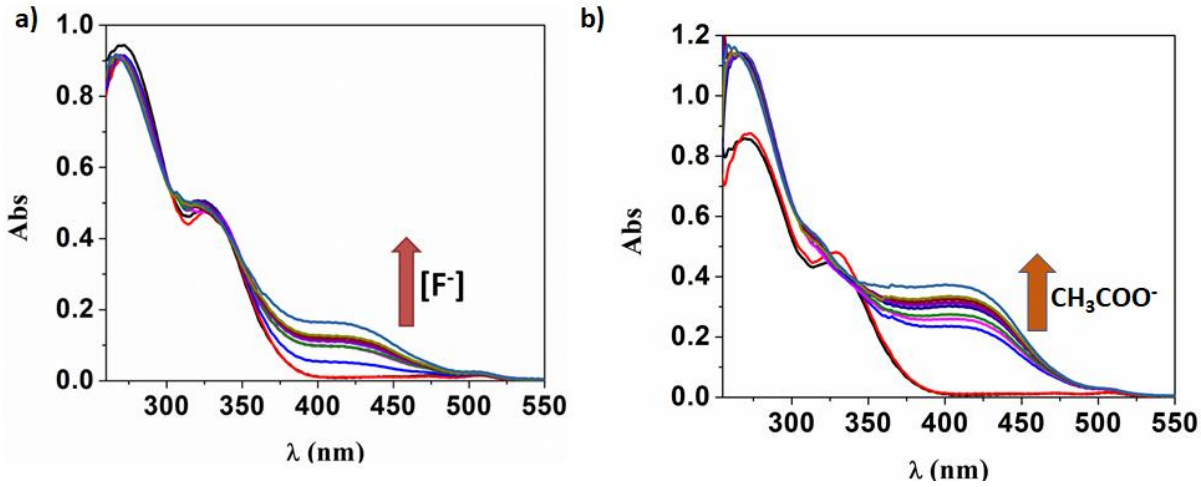

Figure S44: a) Evolution of UV-Vis spectra of **C2** and Ni^{2+} ([**C2**] = 6.2 x 10^{-5} M, [Ni^{2+}] = 7.5 x 10^{-4} M) mixture in DMSO/water upon gradual addition of F^- ion (50 x 10^{-3}M) in DMSO; b) Evolution of UV-Vis spectra of **C2** and Ni^{2+} ([**C2**] = 6.2 x 10^{-5} M, [Ni^{2+}] = 7.5 x 10^{-4} M) mixture in DMSO/water upon gradual addition of CH_3COO^- ion (50 x 10^{-3}M) in DMSO.

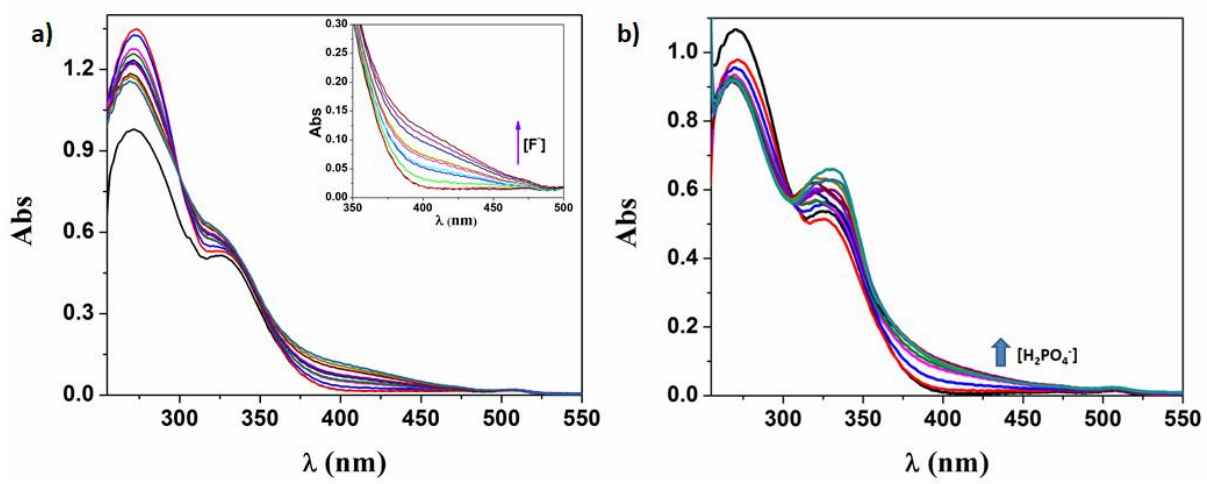

Figure S45: a) Evolution of UV-Vis spectra of **C2** and Cu^{2+} ([**C2**] = 6.2 x 10^{-5} M, [Cu^{2+}] = 3.8 x 10^{-5} M) mixture in DMSO/water upon gradual addition of F^- ion (50 x 10^{-3} M) in DMSO; b) Evolution of UV-Vis spectra of **C2** and Cu^{2+} ([**C2**] = 6.2 x 10^{-5} M, [Cu^{2+}] = 3.8 x 10^{-5} M)) mixture in DMSO/water upon gradual addition of $H_2PO_4^-$ ion (50 x 10^{-3} M) in DMSO.

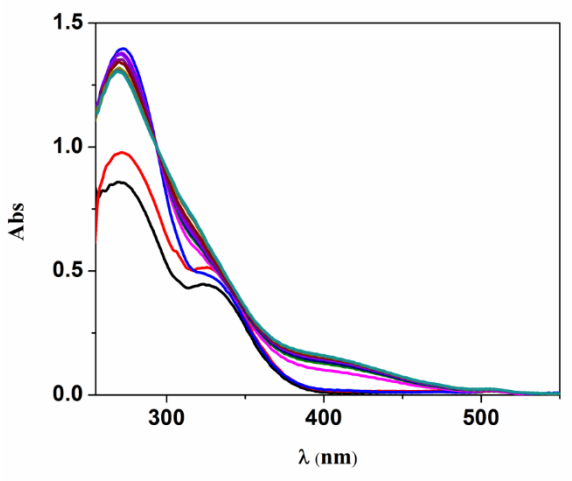

Figure S46: UV-Vis spectra of **C2** and Cu^{2+} ([**C2**] = 6.2 x 10^{-5} M, [Cu^{2+}] = 3.8 x 10^{-5} M) mixture in DMSO/water upon gradual addition of CH_3COO^- ion (50 x 10^{-3} M) in DMSO.

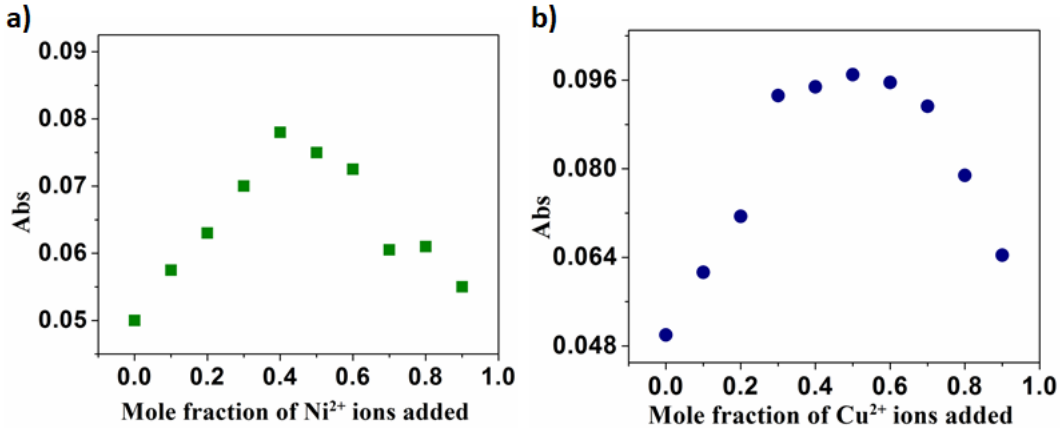

Figure S47: a) Job's plot for **C2.F**$^-$ ([**C2**] = 4.6 x 10^{-5} M, [F^-] = 4.6 x 10^{-5} M) DMSO/water mixture and Ni^{2+} (4.6 x 10^{-5} M) in DMSO; b) Job's plot for **C2.F**$^-$ ([**C2**] = 4.6 x 10^{-5} M, [F^-] = 4.6 x 10^{-5} M) DMSO/water mixture and Cu^{2+} (4.6 x 10^{-5} M) in DMSO.

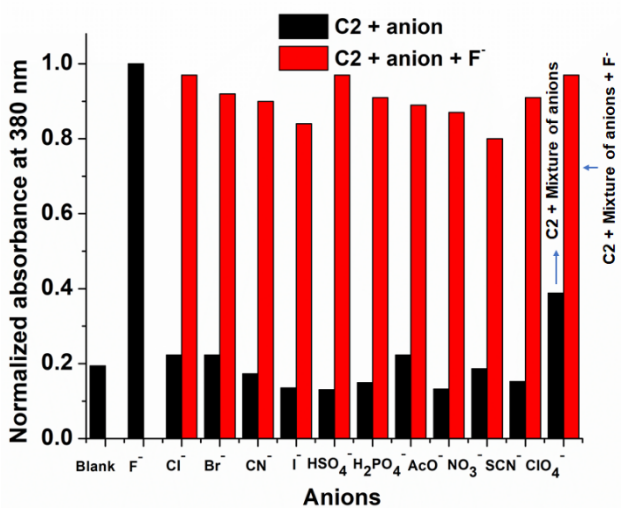

Figure S48: Bar graph of anti-interference performance of **C2** for F^- in presence of other anion solutions in DMSO.

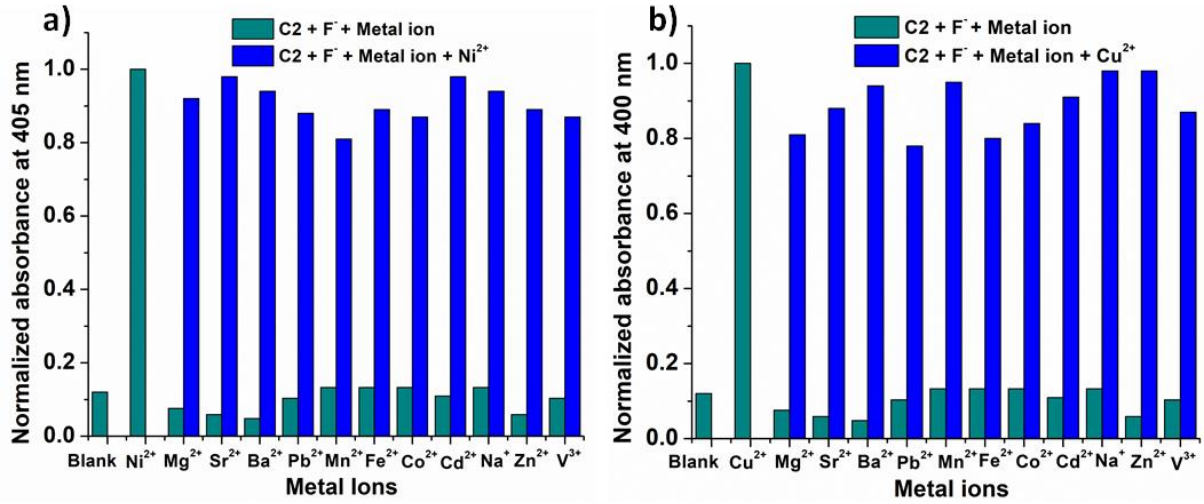

Figure S49: a) Absorption spectrum of **C2** in presence of F^- in DMSO with the presence of various cations (5 equiv.) and Ni^{2+} (5 equiv.) as aqueous salt solutions. The green bars represent the absorption intensity of **C2** in the presence of other metal ions (5 equiv.); the blue bars represent the absorption intensity of **C2** in the presence of the indicated metal ions, followed by 5 equiv. of Ni^{2+} ion; b) Absorption spectrum of **C2** in presence of F^- in DMSO with the presence of various cations (5 equiv.) and Cu^{2+} (5 equiv.) as aqueous salt solutions. The green bars represent the absorption intensity of **C2** in the presence of other metal ions (5 equiv.); the blue bars represent the absorption intensity of **C2** in the presence of the indicated metal ions, followed by 5 equiv. of Cu^{2+} ion.

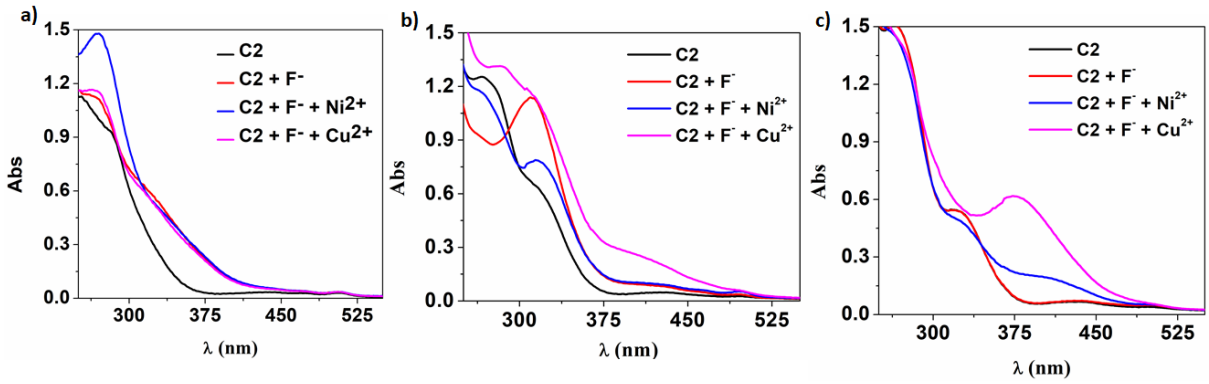

Figure S50: UV-Vis response upon sequential addition of aqueous metal chloride salt solutions ($[Ni^{2+}]$ = 7.5 x 10^{-4} M and $[Cu^{2+}]$ = 3.8 x 10^{-5} M) to **C2.F**$^-$ ([**C2**] = 6.2 x 10^{-5} M, $[F^-]$ = 1.53 x 10^{-3} M) mixture in a) Chloroform ($CHCl_3$) b) Acetonitrile (CH_3CN) and c) methanol (CH_3OH).

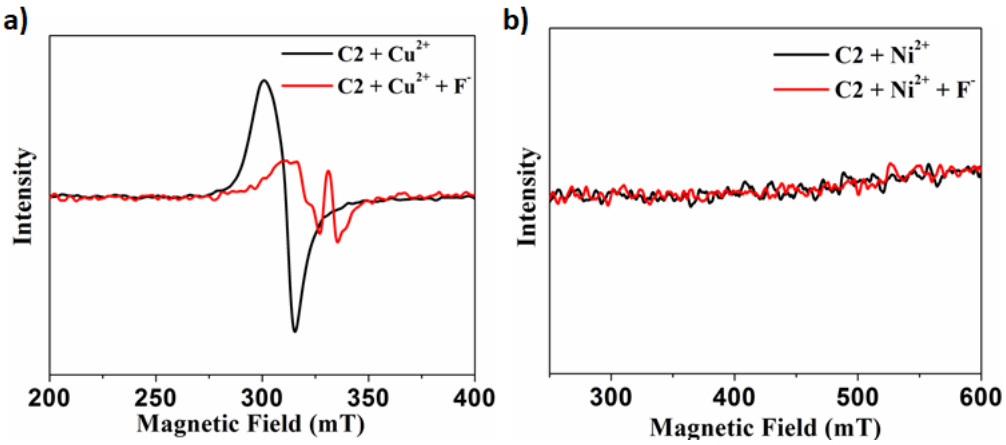

Figure S51: a) EPR spectra (100K, DMSO) [black: addition of $CuCl_2$ (aq) to **C2** solution; red: addition of $CuCl_2.2H_2O$ (aq) to **C2** solution followed by TBAF in DMSO; b) EPR spectra (100K, DMSO) [black: addition of $NiCl_2$ (aq) to **C2** solution; red: addition of $NiCl_2.6H_2O$ (aq) to **C2** solution followed by TBAF in DMSO.

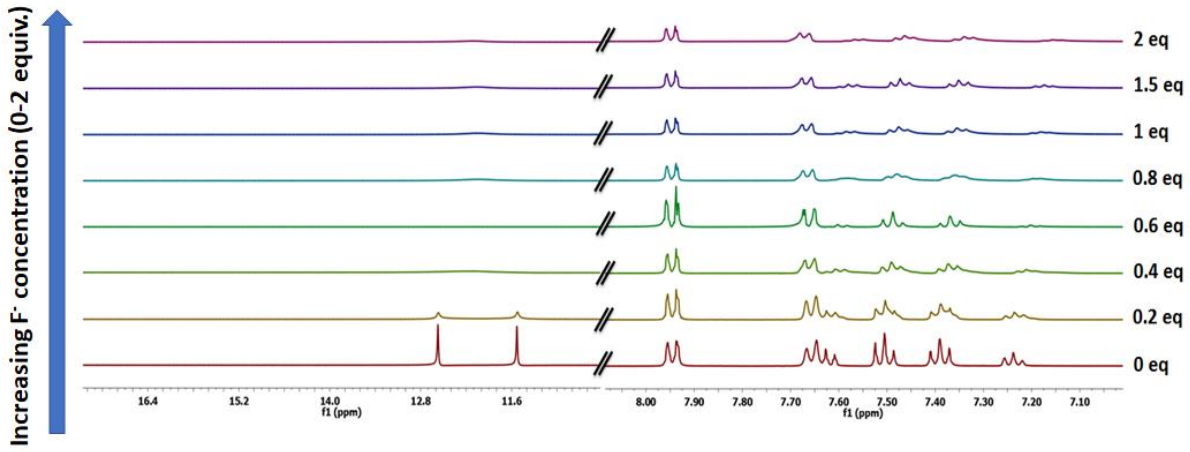

Figure S52: Titration of **C1** (5.62 x 10^{-2} M) with TBAF (0-2 eq.) recorded by ^{1}H NMR spectroscopy (DMSO-d_6, 298 K).

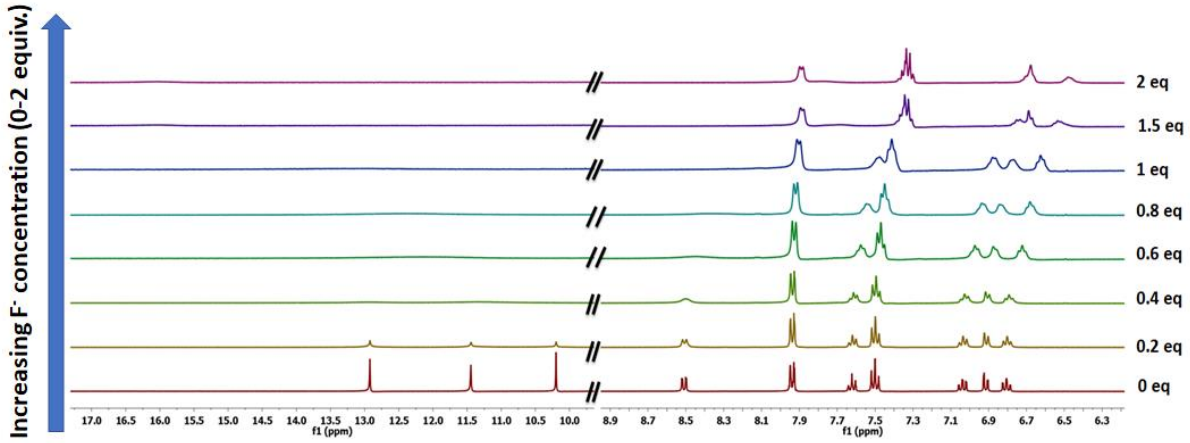

Figure S53: Titration of **C2** (7.32 x 10^{-2} M) with TBAF (0-2 eq.) recorded by ^{1}H NMR spectroscopy (DMSO-d_6, 298K)

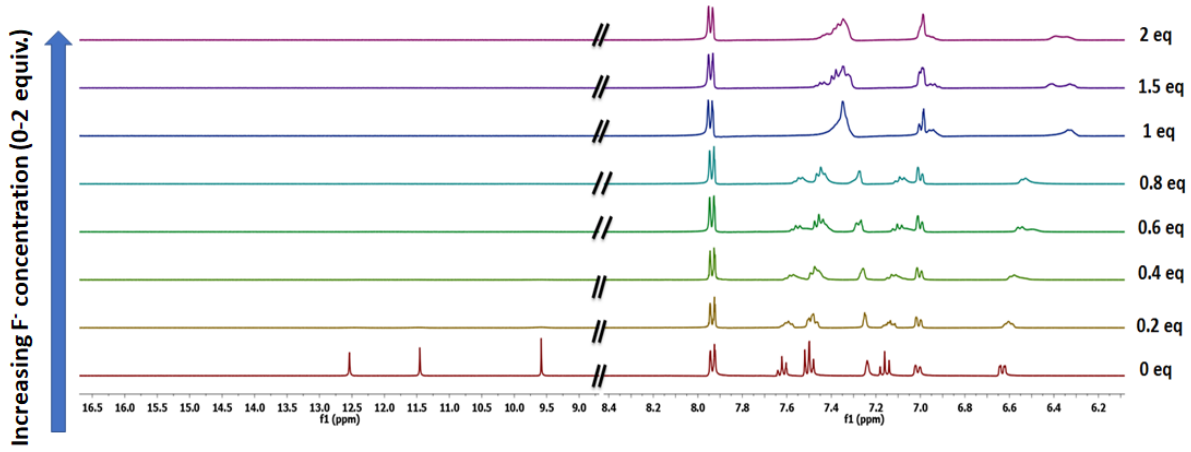

Figure S54: Titration of **C3** (7.32 x 10^{-2} M) with TBAF (0-2 eq.) recorded by ^{1}H NMR spectroscopy (DMSO-d_6, 298 K).

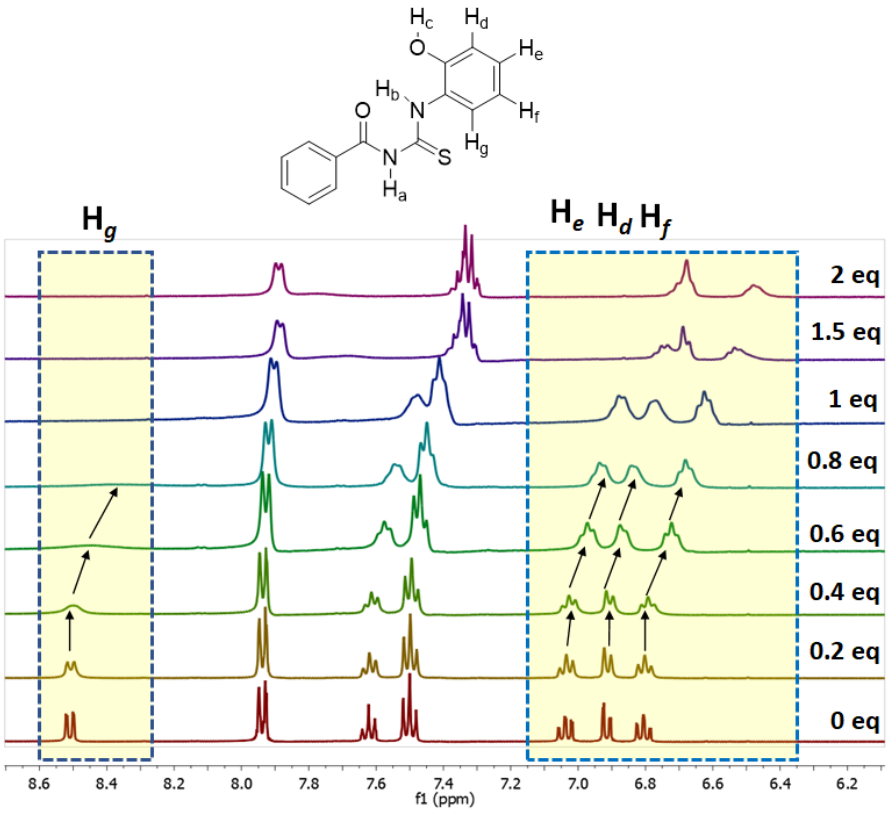

Figure S55: Expanded spectrum (with emphasis on the H_g, H_e, H_d and H_f protons) of titration of **C2** (7.32 x 10^{-2} M) with TBAF (0-2 eq.) recorded by ^{1}H NMR spectroscopy (DMSO-d_6, 298 K).

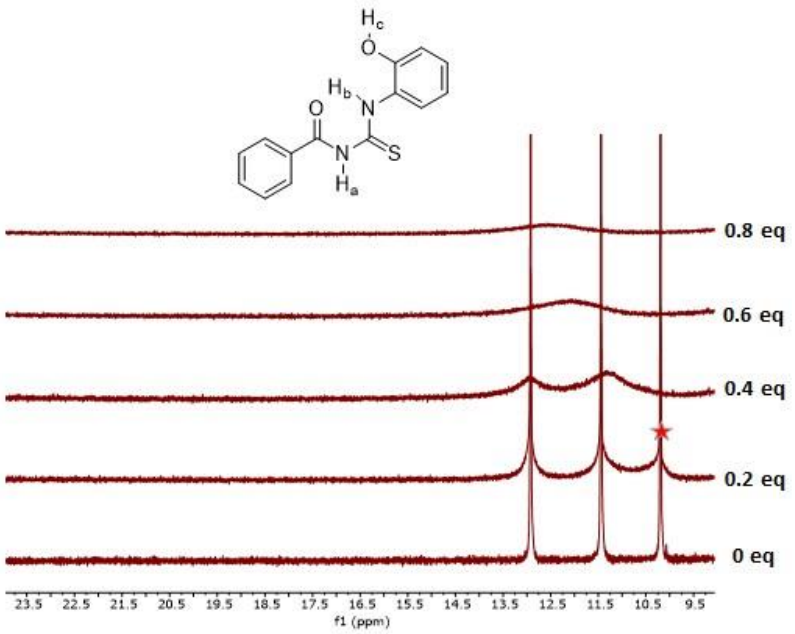

Figure S56: Expanded spectrum (with emphasis on $–OH_c$ proton) of titration of **C2** (7.32 x 10^{-2} M) with TBAF (0-0.8 eq.)recorded by ^{1}H NMR spectroscopy (DMSO-d_6, 298 K).

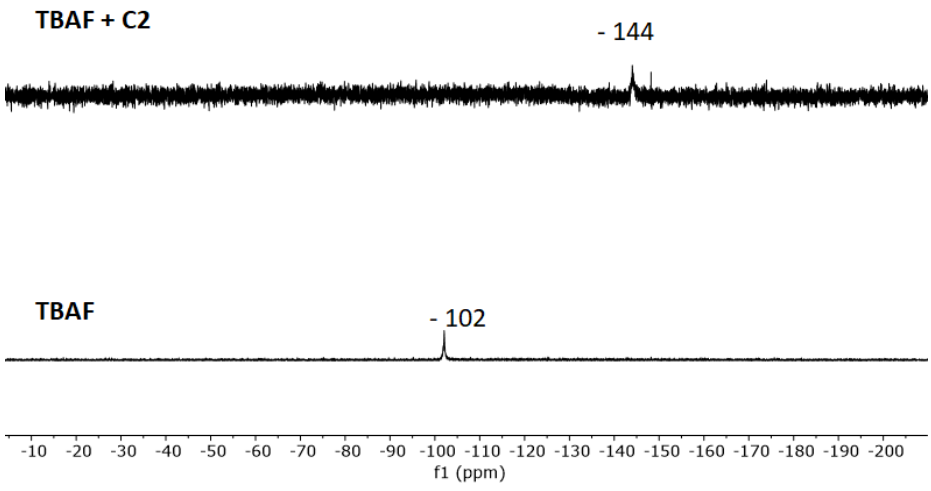

Figure S57: TBAF (2 x 10^{-3} M) in presence of **C2** (1 eq.) recorded by ^{19}F NMR spectroscopy (DMSO-d_6, 298 K).

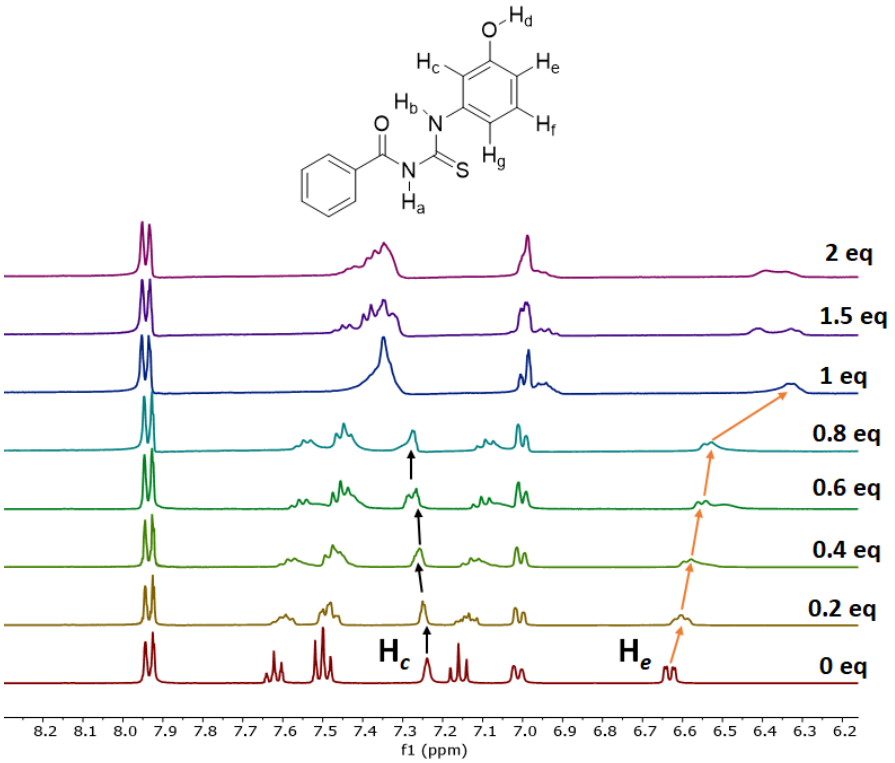

Figure S58: Expanded spectrum (with emphasis on the H_c and H_e protons) of titration of **C3** (7.32×10^{-2} M) with TBAF (0-2 eq.) recorded by ^{1}H NMR spectroscopy (DMSO-d_6, 298 K).

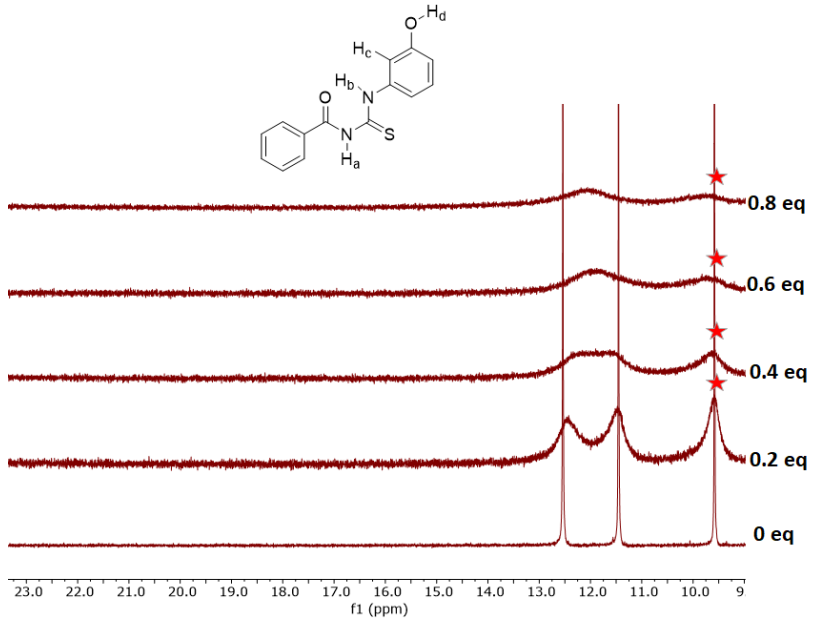

Figure S59: Expanded spectrum (with emphasis on –OH_d proton) of titration of **C2** (7.32×10^{-2} M) with TBAF (0-0.8 eq.) recorded by ^{1}H NMR spectroscopy (DMSO-d_6, 298 K).

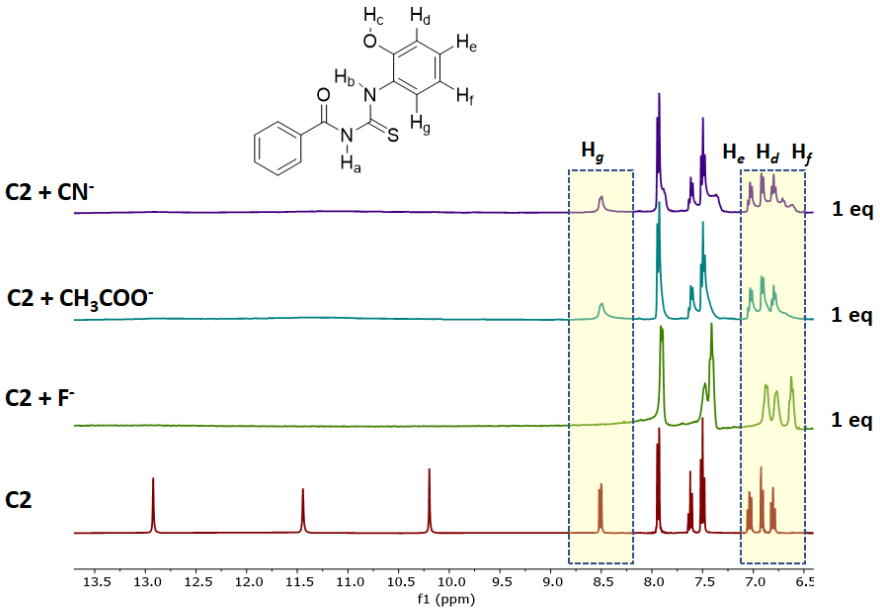

Figure S60: Response of **C2** (7.32 x 10^{-2} M) (with emphasis on H_g, H_e, H_d and H_f protons) in presence of F^-, CN^- and CH_3COO^- recorded by ^1H NMR spectroscopy (DMSO-d_6, 298 K).

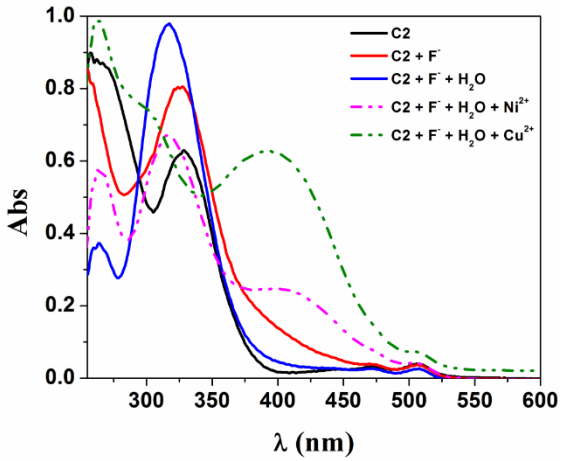

Figure S61: UV-Vis response after sequential addition of H_2O to the **C2**.$\mathbf{F}^-$ ([**C2**] = 6.2 x 10^{-5} M, [F^-] = 1.53 x 10^{-3} M) complex followed by addition of aqueous metal chloride salt ([Ni^{2+}] = 7.5 x 10^{-4} M and [Cu^{2+}] = 3.8 x 10^{-5} M) solution.

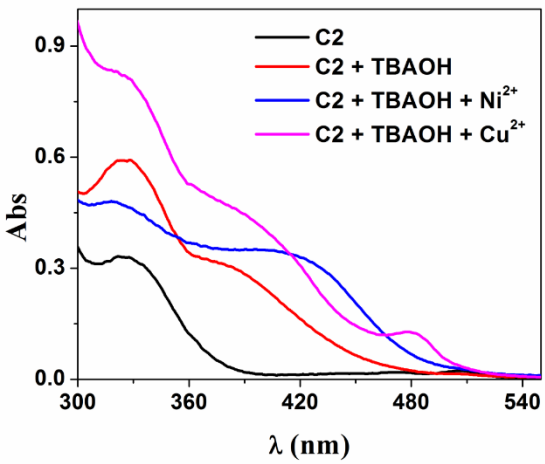

Figure S62: UV-Vis spectrum after sequential addition of TBAOH ([OH^-] = 1.53 x 10^{-3} M) solution to **C2** ([**C2**] = 6.2 x 10^{-5} M) in DMSO followed by addition of aqueous metal salt ($NiCl_2.6H_2O$ /$CuCl_2.2H_2O$) solution.

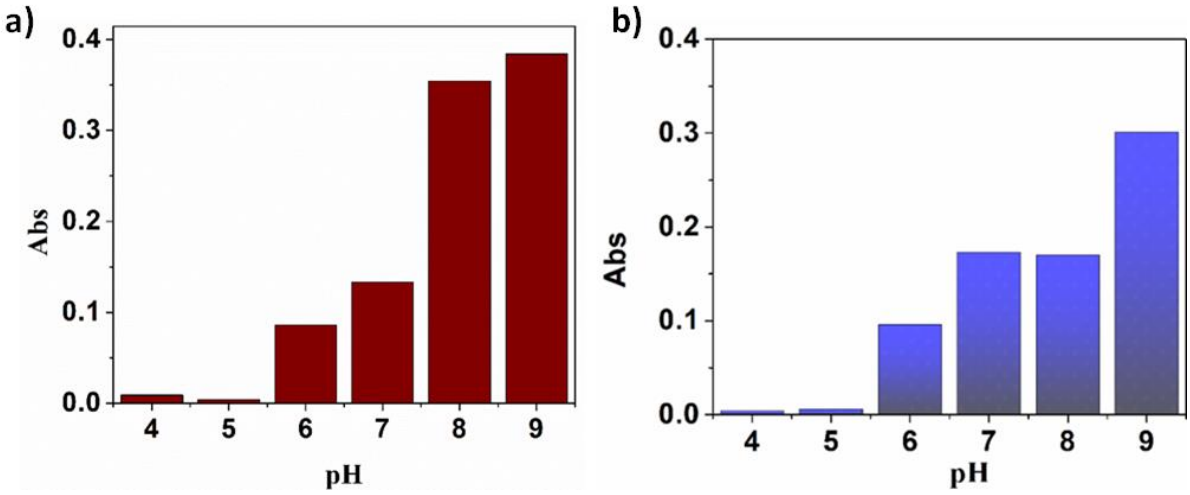

Figure S63: a) Study on effect of pH on fluoride sensing by **C2** in presence of aqueous $NiCl_2$ in HEPES buffer (DMSO:Water = 7:3, pH = 7.2) at λ_{max} = 415 nm; b) Study on effect of pH on fluoride sensing by **C2** in presence of aqueous $CuCl_2$ in HEPES buffer (DMSO:Water = 7:3, pH = 7.2) at λ_{max} = 425 nm.

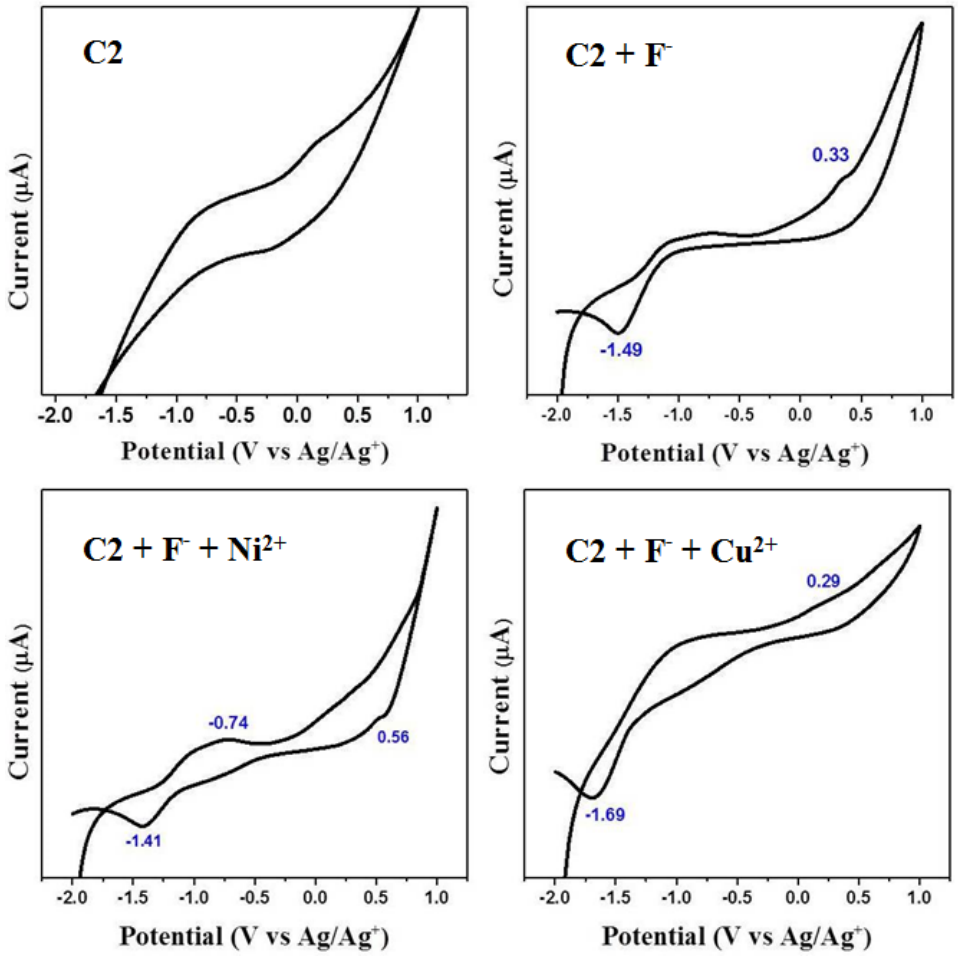

Figure S64: Cyclic Voltammogram recorded in *n*-Bu_4NClO_4/DMSO: a) **C2** in DMSO; b) **C2** + TBAF in DMSO; c) **C2** + TBAF + $NiCl_2.6H_2O$ in DMSO/H_2O mixture; d) **C2** + TBAF + $CuCl_2.2H_2O$ in DMSO/H_2O mixture.

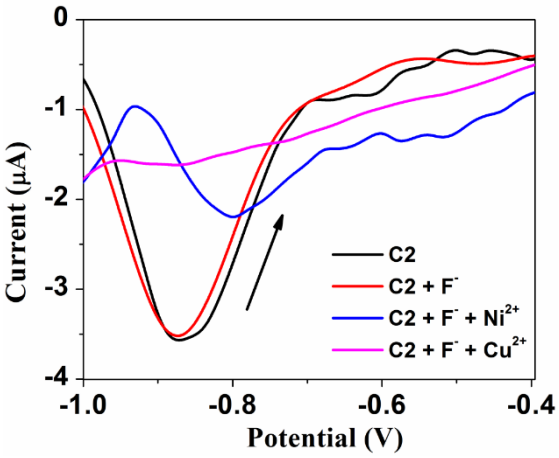

Figure S65: Changes in the DPV (vs Ag/Ag^{+}) curves w.r.t. the ligand based peak of **C2** in presence of *n*-Bu_4NClO_4 (0.1 M) upon sequential addition TBAF solution followed by aqueous metal salt solution to a **C2** solution in DMSO. Changes in the curves (Black: **C2** solution in DMSO; red: **C2** + TBAF in DMSO; blue: **C2** + TBAF + $NiCl_2$ in DMSO/water mixture; pink: **C2** + TBAF + $NiCl_2$ in DMSO/water mixture).

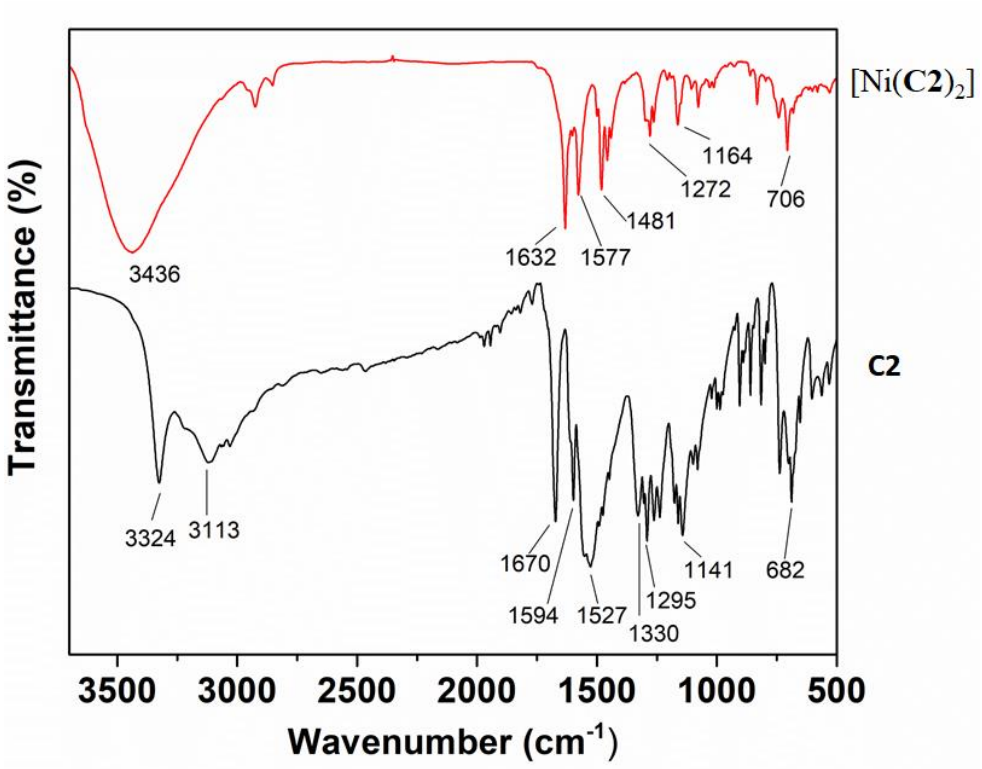

Figure S66: IR spectrum of **C2** and [Ni(**C2**)$_2$] collected in ATR mode.

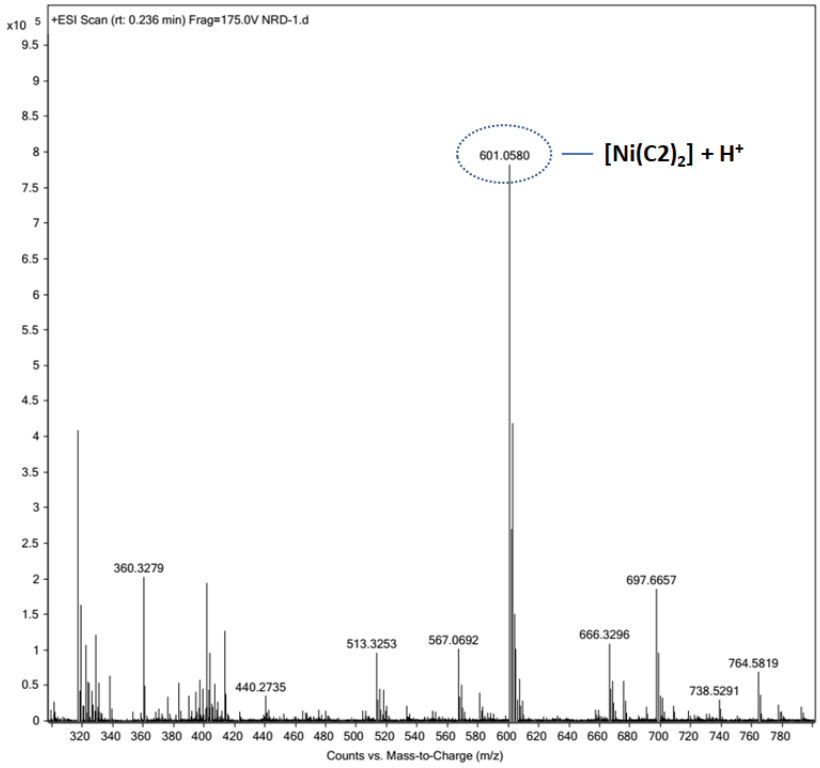

Figure S67: ESI mass spectra of [Ni(**C2**)$_2$].

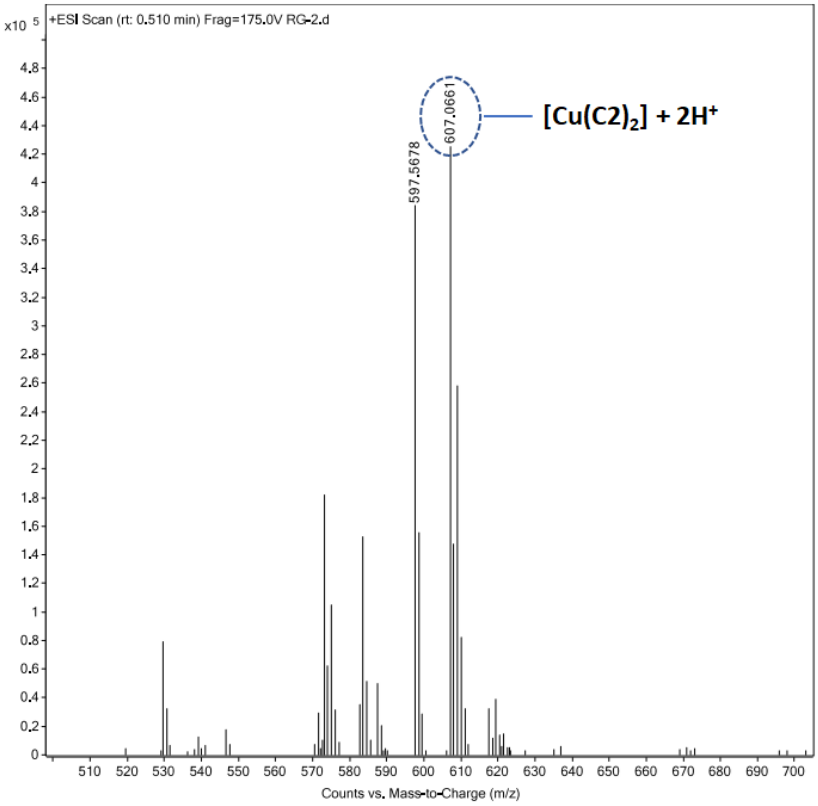

Figure S68: ESI mass spectra of [Cu(**C2**)$_2$].

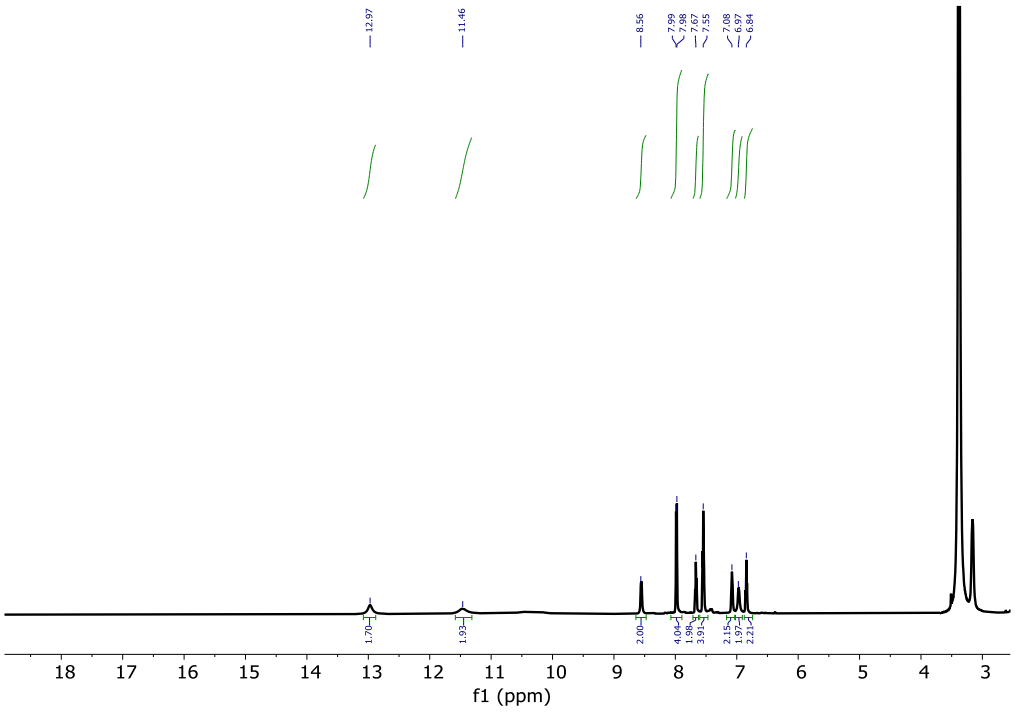

Figure S69: ^{1}H NMR spectrum of *in situ* metal complex formed for **C2** (7.32 x 10^{-2} M) in presence of Ni^{2+} ions (0.5 equiv.) and F^{-} (0.5 equiv.) in DMSO-d_6 at 298K.

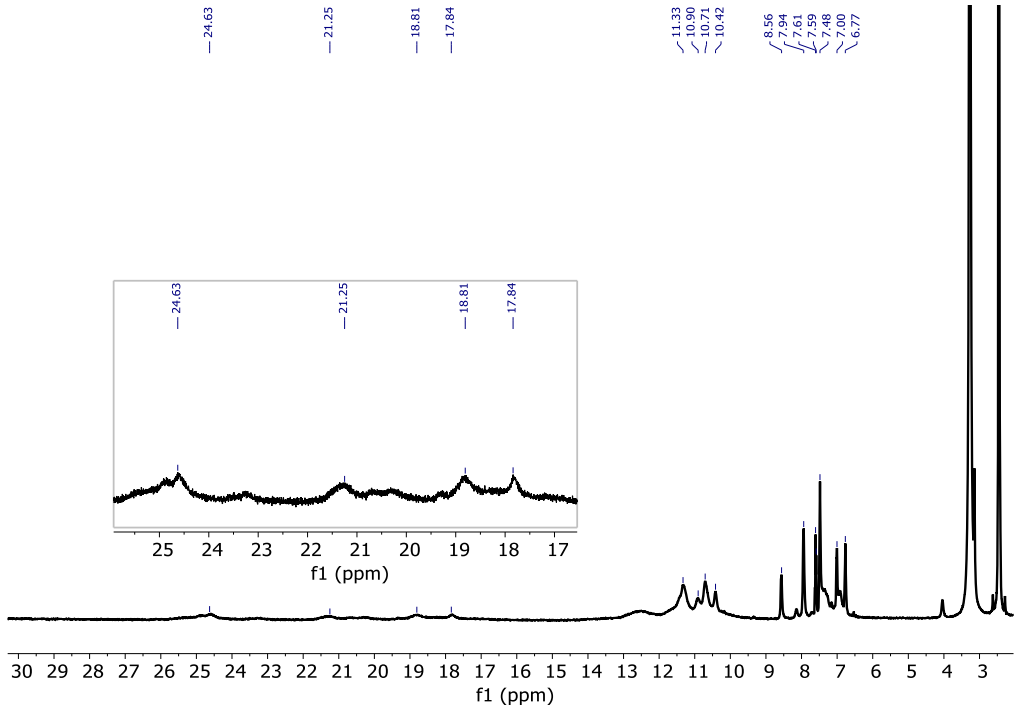

Figure S70: ^{1}H NMR spectrum of *in situ* metal complex formed for **C2** (7.32 x 10^{-2} M) in presence of Cu^{2+} ions (0.5 equiv.) and F^{-} (0.5 equiv.) in DMSO-d_6 at 298K.

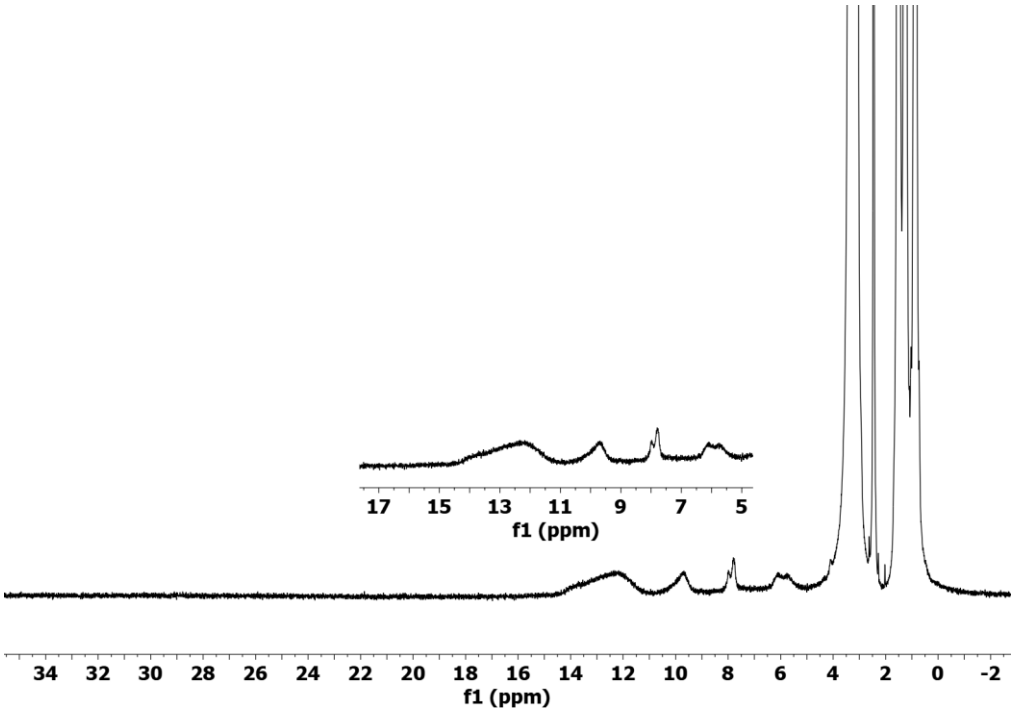

Figure S71: ^{1}H NMR spectrum of the isolated yellow Cu(II) complex in DMSO-d_6 at 298K.

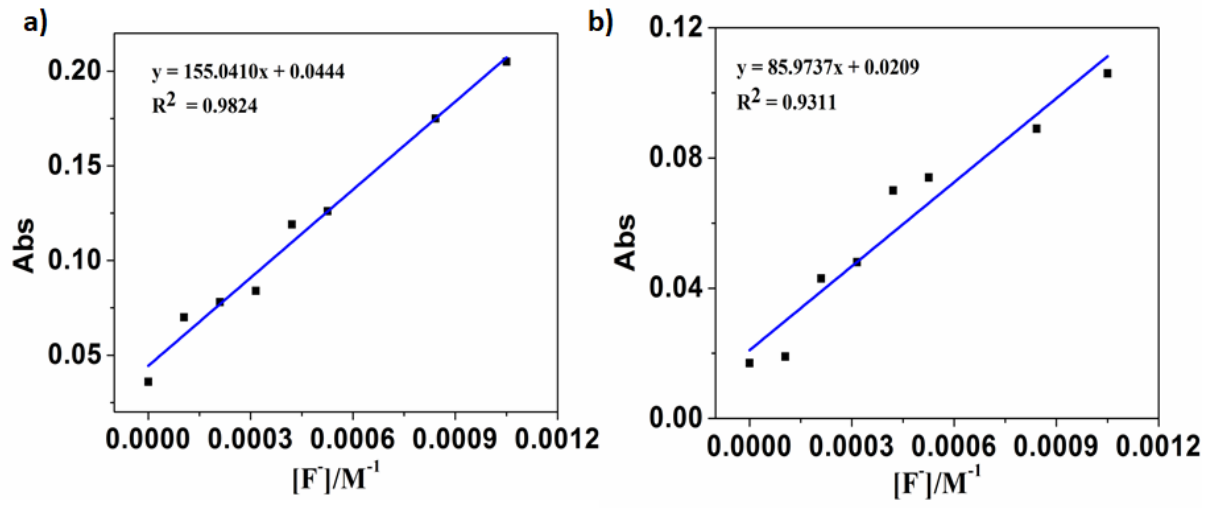

Figure S72: a) Calibration curve for determining the concentration of fluoride (as NaF in H_2O) in a sample λ_{max} = 406 nm. [**C2**] = 6.2 x 10^{-5} M; [Cu^{2+}] = 7.5 x 10^{-5} M; b) Calibration curve for determining the concentration of fluoride (as NaF in H_2O) in a sample at λ_{max} = 420 nm. [**C2**] = 6.2 x 10^{-5} M; [Ni^{2+}] = 7.5 x 10^{-5} M.

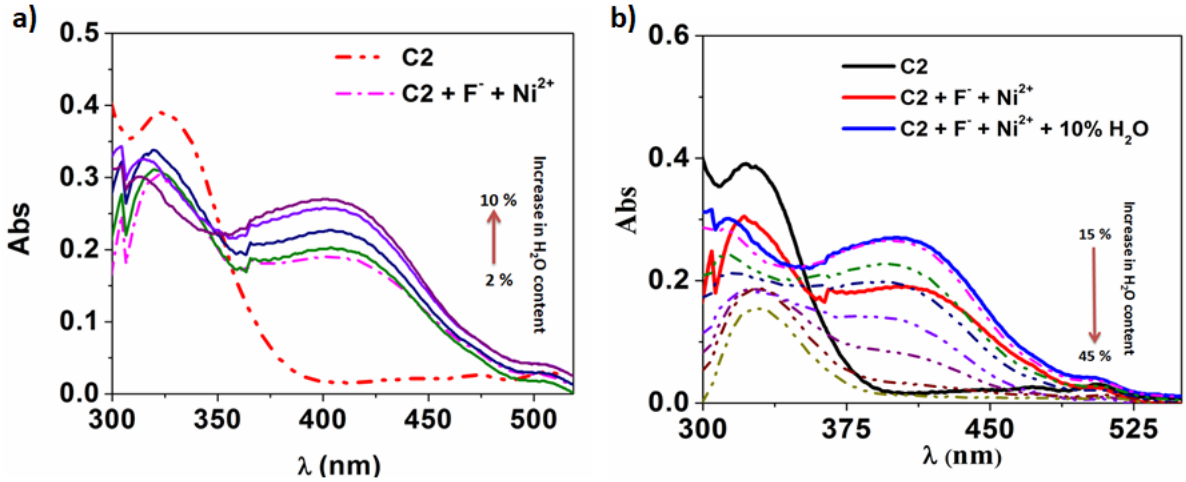

Figure S73: a) UV-Vis spectra of (**C2** + F^-+ Ni^{2+}) ([**C2**] = 6.2 x 10^{-5} M, [F^-] = 1.53 x 10^{-3} M, [Ni^{2+}] = 7.5 x 10^{-4} M) showing initial increase in the absorbance at λ_{max} = 404 nm upon addition of H_2O (upto 10% of total volume); b) UV-Vis spectra of (**C2** + F^-+ Ni^{2+}) ([**C2**] = 6.2 x 10^{-5} M, [F^-] = 1.53 x 10^{-3} M, [Ni^{2+}] = 7.5 x 10^{-4} M) showing subsequent decrease in the absorbance (represented by dotted lines) at λ_{max} = 404 nm after addition of H_2O (10% onwards).

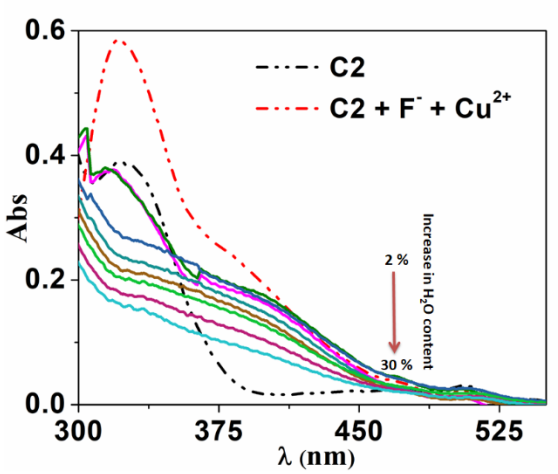

Figure S74: UV-Vis spectra of (**C2** + F^- + Cu^{2+}) ([**C2**] = 6.2 x 10^{-5} M, [F^-] = 1.53 x 10^{-3} M, [Cu^{2+}] = 3.8 x 10^{-5} M) showing decrease in the absorbance at λ_{max} = 374 nm upon addition of H_2O.

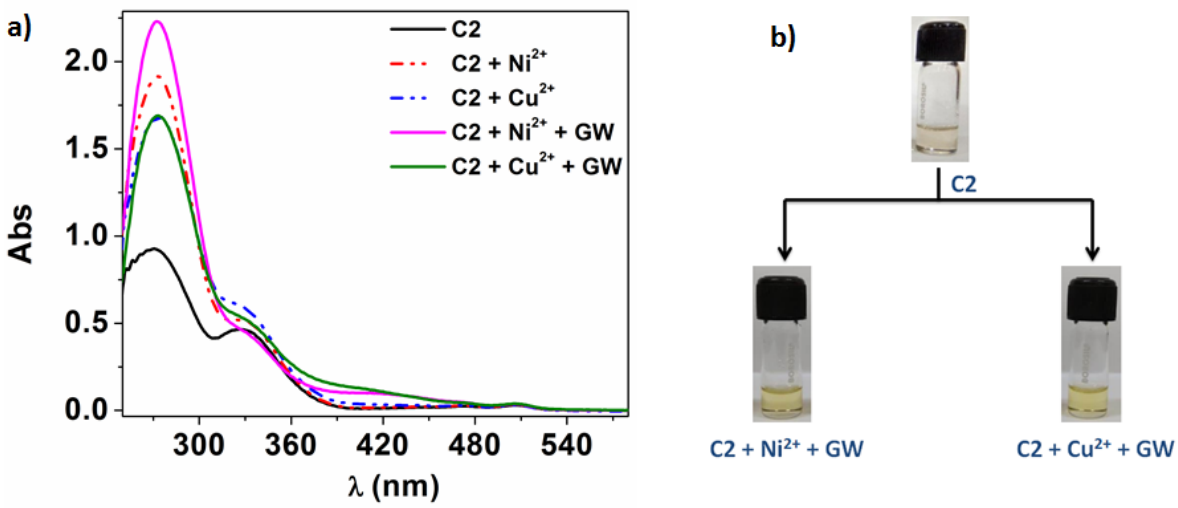

Figure S75: a) UV-Vis spectra upon sequential addition of groundwater samples (GW) to **C2** ([**C2**] = 6.2 x 10^{-5} M) in DMSO in presence of aqueous Ni^{2+} ([Ni^{2+}] = 7.5 x 10^{-4} M) ions and Cu^{2+} ions ([Cu^{2+}] = 3.8 x 10^{-5} M). b) Colour change observed upon addition of 20 µL groundwater samples (GW) to **C2** in DMSO in presence of aqueous Ni^{2+} ions and Cu^{2+} ions.

Table S2: Literature reports on transition metal based fluoride sensor

S. No.	Metal receptor system	Fluoride Salt	LOD	Solvent used for study	Reference
1	Copper(II) bis(terpyridine) complex	TBAF	5.07 µM	Acetonitrile	P. K. Kar and co-workers, *Photochem. Photobiol. Sci.*, 2018, **17**, 815-821.
2	Co(II) Hexacarboxamide Cryptand Complex	TBAF	2-5 ppm	DMF	C. C. Cummins and co-workers, *Inorg. Chem.* 2017, **56**, 7615−7619.
3	Zn(II) tripodal complex	TBAF/ NaF	4.84×10^{-12} M	Water	N. Singh and co-workers, *Dalton Trans.*, 2015, **44**, 12589-12597.
4	2,4-dihydroxybenzaldoxime complex of Cu(II), Ni(II) and Zn(II)	TBAF	4.86×10^{-6} M	DMSO	J. B. Baruah and co-workers, *RSC Adv.*, 2015, **5**, 82144-82152.
5	Ru(II) complex	TBAF	-	Acetonitrile	G. K. Lahiri and co-workers, *Dalton Trans.*, 2012, **41**, 4484-4496.
6	Fe(III) complex	NaF	140 µM	DMSO/Water (3:7)	Z. Shen and co-workers, *Tetrahedron*, 2011, **67**, 7909-7912.
7	Co(II) thiazoline based complex	NaF	-	DMF/water (9:1)	C.-S. Ha and co-workers, *Dalton Trans.*, 2009, **47**, 10422-10425.
8	Zr(IV) EDTA flavonol complex	NaF	3×10^{-6} M	Water	T. M. Suzuki and co-workers, *J. Chem. Soc.*,

					Perkin Trans. 2, 2002, 759–762.
9	Zn(II)Terpyridine−Triarylborane Conjugates	TBAF	-	THF	M. H. Lee and co-workers, *Organometallics*, 2014, **33**, 753–762.
10	Ru(II)-bipy based complex	TBAF	1 ppm-10 ppm	Acetonitrile	Z. Bai and co-workers, *Dalton Trans.*, 2006, **30**, 3678–3684.
11	amino-naphthoquinone based Co(II), Ni(II), Cu(II), and Zn(II) complexes	TBAF	0.006 µM	DMF/water (3:7)	K. P. Elango and co-workers, *RSC Adv.*, 2016, **6**, 91265–91274.
12	Cu(I) Schiff base complex	TBAF/ NaF	0.12 µM	DMSO/Water	S. P. Mahanta.and co-workers, *New J. Chem.*, 2018, **42**, 3758-3764.
13	Cu(I) DPQ complex	TBAF/ NaF	0.15 ppm	DMSO/Water	S. P. Mahanta.and co-workers, *New J. Chem.*, 2019, **43**, 3447-3453
14	Al(III) Schiff base complex	TBAF/ KF	2×10^{-12} M	Water	P. Mal and co-workers, *Dalton Trans.*, 2021, 50, 3027-3036
15	**This work**	**TBAF/ NaF**	**1.07 ppm**	**DMSO/Water**	

Theoretical Studies:

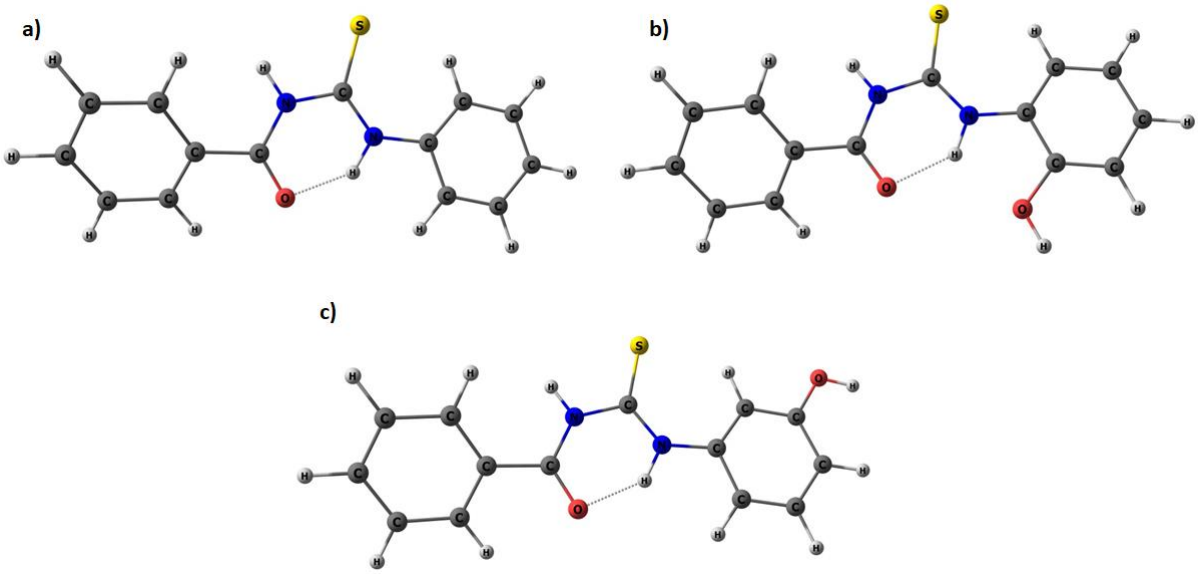

Figure S76: DFT optimized structure of a) **C1**, b) **C2**, c) **C3**.

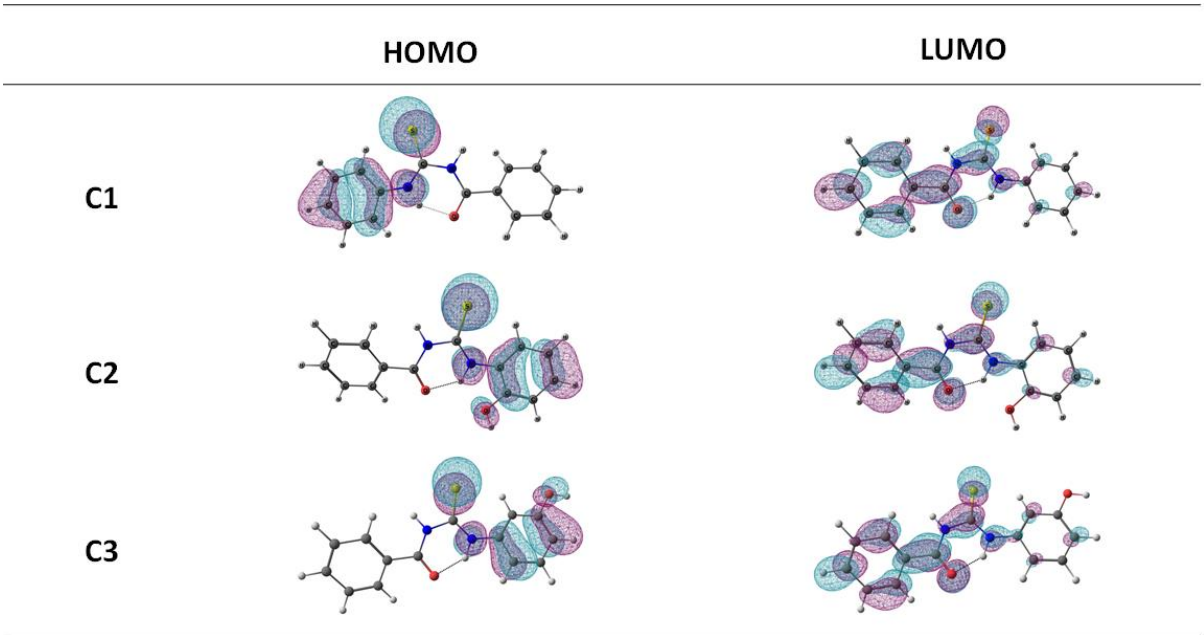

Figure S77: HOMO and LUMO of **C1**, **C2** and **C3**.

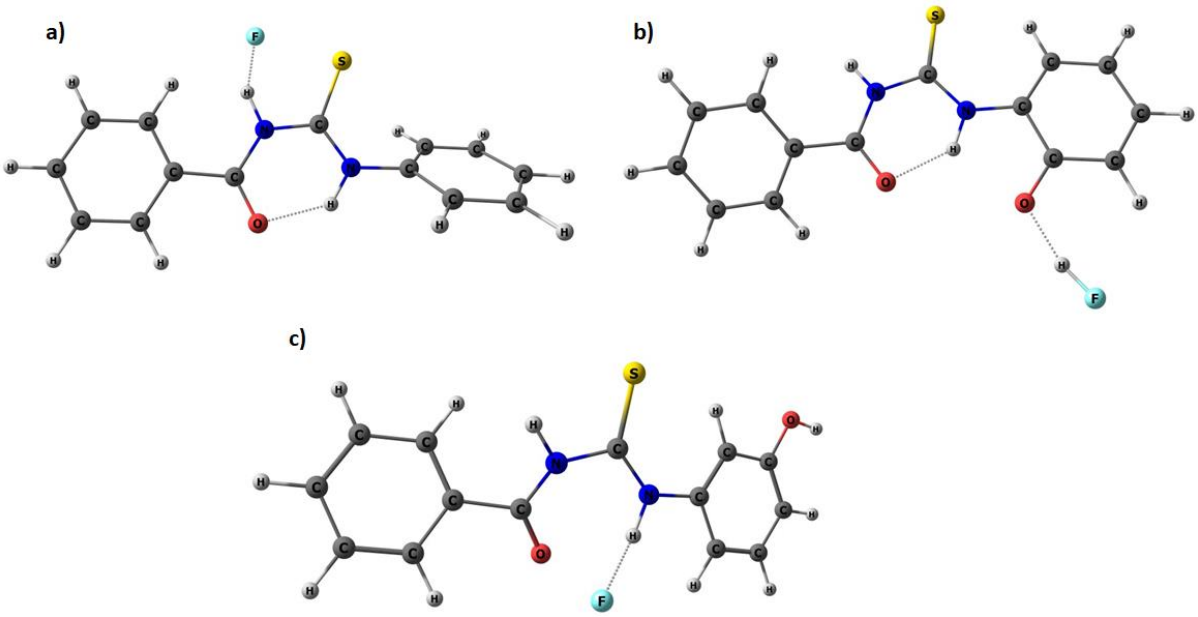

Figure S78: Structures for interaction of F^- with a) **C1**, b) **C2** and c) **C3**

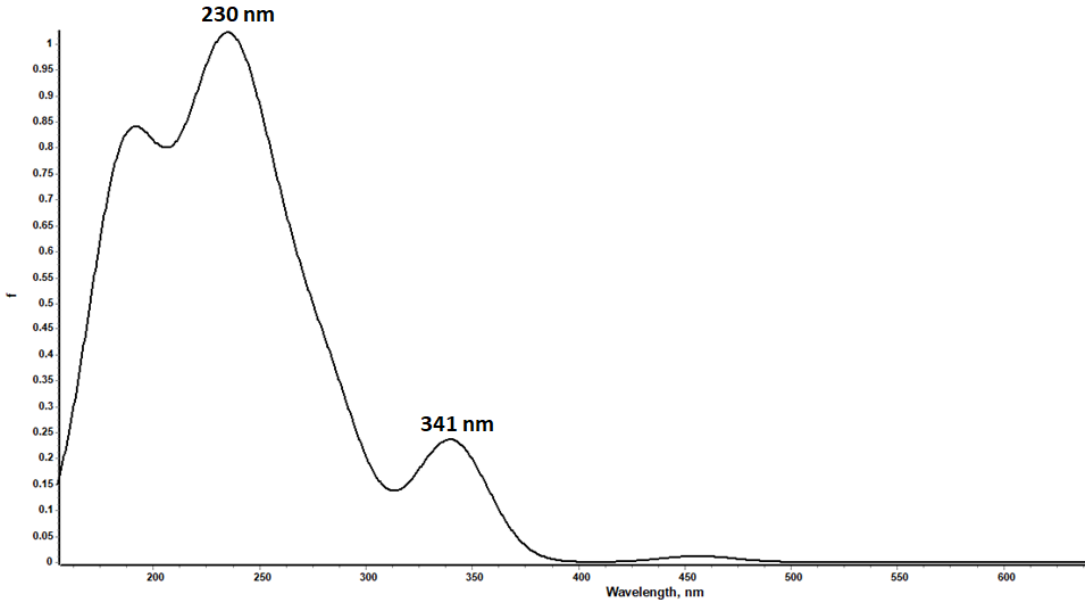

Figure S79: UV-Vis spectrum of **C2**.F^- complex simulated from the TD- DFT calculation.

395.96	0
355.26	0
345.92	0
333.61	0
326.3	0.0002
290.82	0
284.03	0
279.83	0
277.93	0.4567
267.41	0
265.6	0
259.29	0.09
254.09	0
249.28	0.6141
246.02	0.0846
245.55	0
239.13	0.0403
233.83	0
230.91	0
222.99	0.0531
213.4	0.0844
211.07	0
209.21	0.0124
207.6	0
204.23	0.1537

Table S3: TD f –values of the obtained UV-Vis spectrum for **C2**.F^- complex.

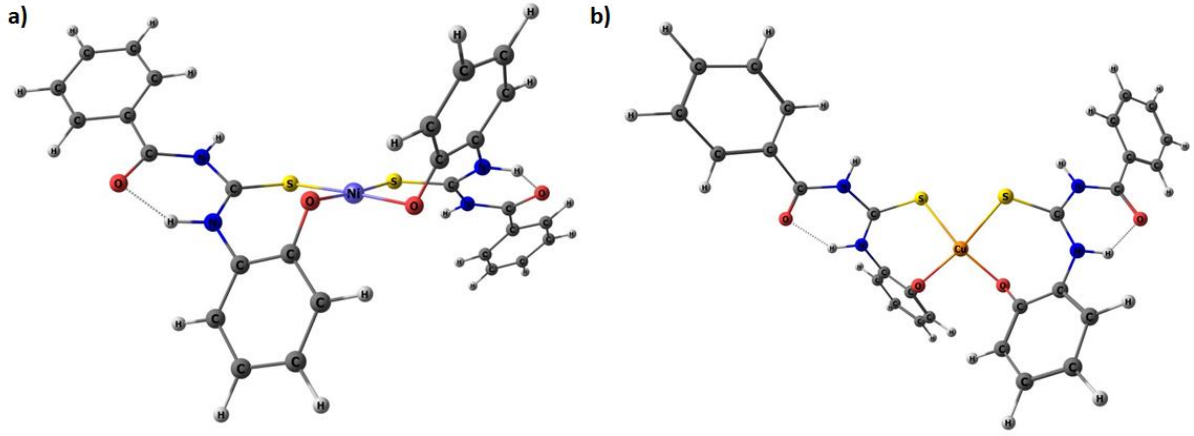

Figure S80: DFT optimized structure of a) [Ni(**C2**)$_2$] and b) [Cu(**C2**)$_2$] complex.

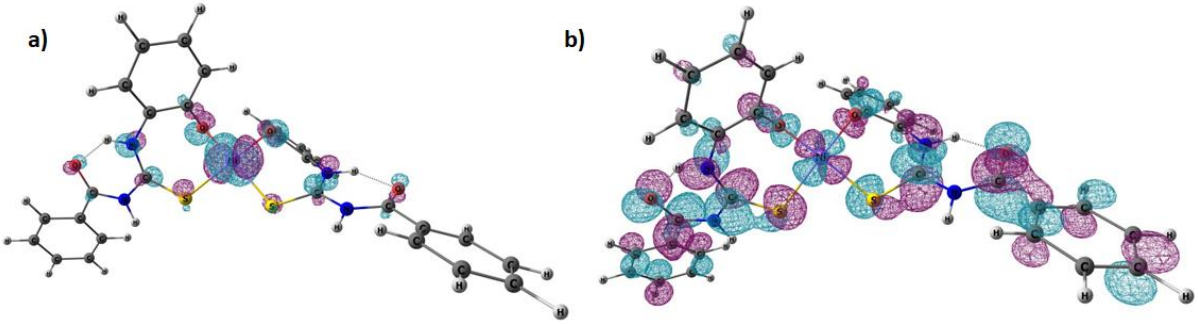

Figure S81: a) HOMO and b) LUMO of [Ni(**C2**)$_2$] complex

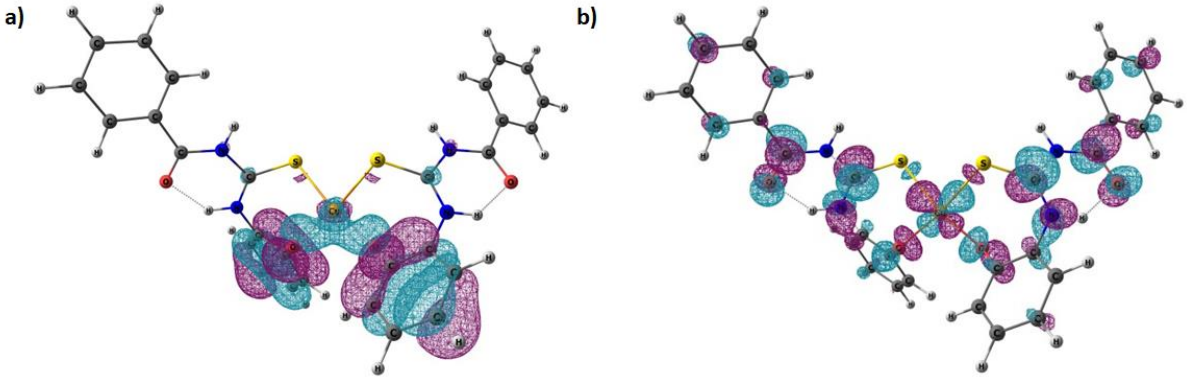

Figure S82: a) HOMO and b) LUMO of [Cu(**C2**)$_2$] complex

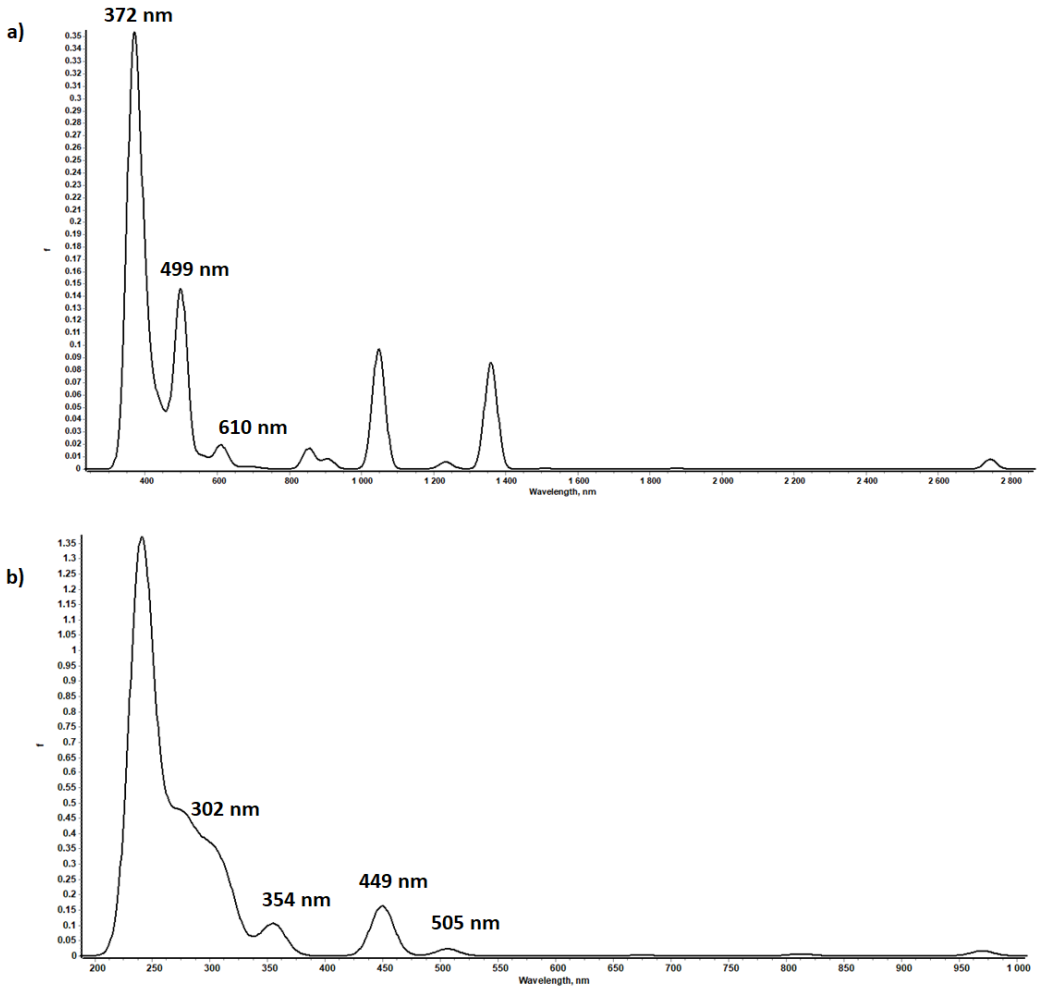

Figure S83: UV-Vis spectrum of a) [Ni(**C2**)2] and b) [Cu(**C2**)2] complex simulated from the TD-DFT calculation

716.67	0.0008
686.64	0.0017
642.72	0.002
610.41	0.0186
589.84	0.0002
588.32	0.0012
565.22	0.0011
562.08	0.0002
557.99	0.007
549.41	0.0015
547.57	0.0004
526.71	0.0013
499.89	0.1401
481.3	0.0054
474.69	0.0006
471.64	0.0048

467.79	0.0023
450.87	0.012
447.62	0.0042
445.4	0.0076
441.6	0.0089
439.88	0.0003
439.54	0.0001
432.61	0.0011
429.2	0.0056
424.29	0.0076
415.56	0.0217
414.71	0.0026
407.51	0.003
405.27	0.0005
397.46	0.0219
395.47	0.0309
392.64	0.004
388.57	0.0418
378.09	0.0034
375.58	0.028
372.69	0.022
371.77	0.0026
369.37	0.1499
366.63	0.0006
365.55	0.0017
360.86	0.0742
359.2	0.0037
358.33	0.0455

Table S4:TD f –values of the obtained UV-Vis spectrum for [Ni(**C2**)$_2$]

671.97	0.0001
505.85	0.0231
469.63	0.0014
449.48	0.1634
361.49	0.0235
360.72	0.0003
354.92	0.0031
354.51	0.0743
348.87	0.0001
346.18	0.0069
338.52	0.0159
332.68	0.009
328.3	0.0013

315.59	0.0841
315.43	0.0915
302.04	0.1404
300.72	0.0627
300.56	0.0018
296.36	0.0091
295.74	0.0123
293.57	0.0025
291.48	0.0453
289.31	0.0058
288.13	0.0081
287.81	0.0609
283.54	0.0297
282.11	0.0196
278.39	0.1647
274.89	0.0612
274.6	0.0216
273.26	0.003
268.35	0.0223
267.61	0.0041
266.56	0.0696
265.76	0.0068
263.19	0.0266
261.18	0.0793
260.28	0.0457
258	0.0297
254.75	0.0167
254.65	0.009
250.64	0.0708

Table S5:TD f –values of the obtained UV-Vis spectrum for [Cu(**C2**)$_2$]

Z-matrix of the Ligand **C1**

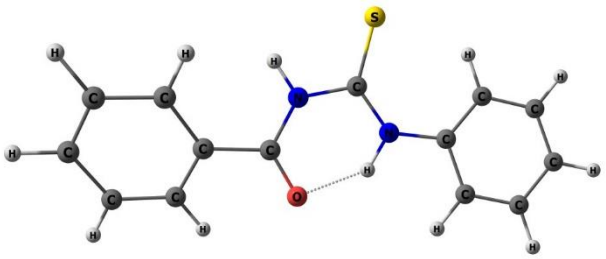

C	-5.767244000	-0.274963000	0.090635000
C	-5.036419000	0.852362000	0.496190000
C	-3.636432000	0.833208000	0.458242000
C	-2.960970000	-0.319169000	0.013103000
C	-3.696043000	-1.453777000	-0.374229000
C	-5.094704000	-1.429349000	-0.340979000
C	-1.471789000	-0.414705000	-0.043540000
N	-0.778611000	0.780040000	-0.128689000
C	0.621015000	1.010659000	-0.117941000
N	1.367259000	-0.111822000	-0.052440000
C	2.774446000	-0.309205000	0.007973000
C	3.743613000	0.705087000	-0.077599000
C	5.103271000	0.363586000	-0.007706000
C	5.511030000	-0.967799000	0.143728000
C	4.538320000	-1.977837000	0.226129000
C	3.181757000	-1.652431000	0.159013000
O	-0.882343000	-1.526699000	-0.030479000
S	1.109633000	2.644895000	-0.185242000
H	-6.851349000	-0.256351000	0.119757000
H	-5.552981000	1.738004000	0.848538000
H	-3.094016000	1.704034000	0.814860000
H	-3.159073000	-2.340288000	-0.692459000
H	-5.657356000	-2.304305000	-0.646581000
H	-1.301568000	1.640501000	-0.229774000
H	0.816435000	-0.978943000	-0.035345000
H	3.446316000	1.737031000	-0.195652000
H	5.844984000	1.152532000	-0.073543000
H	6.565288000	-1.216172000	0.197569000

H	4.834701000	-3.014503000	0.344227000
H	2.433598000	-2.437806000	0.225892000

Z-matrix of the Ligand **C2**

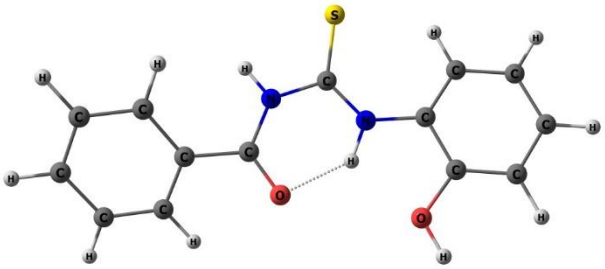

C	3.091787000	-0.268864000	-0.009935000
C	3.807712000	-1.412493000	0.386130000
H	3.254867000	-2.285466000	0.714610000
C	5.206529000	-1.414615000	0.347189000
H	5.754092000	-2.296865000	0.659433000
C	5.898933000	-0.277411000	-0.098648000
H	6.983117000	-0.279407000	-0.132172000
C	5.187197000	0.858822000	-0.512740000
H	5.718389000	1.731396000	-0.875989000
C	3.786922000	0.865757000	-0.469268000
H	3.258790000	1.742582000	-0.832455000
C	1.599177000	-0.338926000	0.051805000
C	-0.456433000	1.140216000	0.125920000
C	-2.661825000	-0.055650000	0.002700000
C	-3.593123000	0.992862000	0.035038000
H	-3.248036000	2.013412000	0.111206000
C	-4.968910000	0.714976000	-0.030874000
H	-5.673712000	1.538194000	-0.005373000
C	-5.430822000	-0.601544000	-0.128212000
H	-6.493517000	-0.809904000	-0.180321000
C	-4.508999000	-1.660463000	-0.159078000
H	-4.852784000	-2.688467000	-0.234323000

C	-3.144256000	-1.382849000	-0.093310000
H	-2.503409000	-3.269869000	-0.185588000
H	1.476073000	1.720523000	0.236368000
H	-0.766528000	-0.860863000	0.035197000
N	0.932237000	0.873102000	0.134865000
N	-1.248877000	0.050862000	0.056482000
O	-2.159675000	-2.365181000	-0.116037000
O	0.988800000	-1.434463000	0.045115000
S	-0.887950000	2.794702000	0.202316000

Z-matrix of the Ligand **C3**

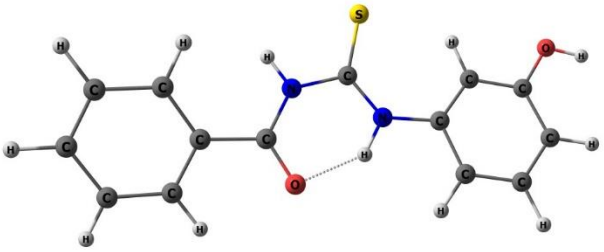

C	3.316521000	-0.272441000	-0.013162000
C	3.943287000	0.904745000	-0.464467000
H	3.364495000	1.750675000	-0.823822000
C	5.341206000	0.981169000	-0.504959000
H	5.820670000	1.885446000	-0.862385000
C	6.118106000	-0.113545000	-0.095692000
H	7.200474000	-0.050312000	-0.126593000
C	5.494288000	-1.292670000	0.342161000
H	6.093081000	-2.142193000	0.650888000
C	4.097787000	-1.374515000	0.377661000
H	3.598125000	-2.280901000	0.700682000
C	1.832389000	-0.426798000	0.045314000
C	-0.312853000	0.919950000	0.122326000
C	-2.411883000	-0.483371000	-0.014704000
C	-3.409758000	0.497645000	0.042298000

H	-3.176998000	1.547688000	0.140679000
C	-4.753202000	0.100550000	-0.029850000
C	-5.119963000	-1.245827000	-0.156005000
H	-6.165443000	-1.536045000	-0.211917000
C	-4.106864000	-2.215669000	-0.210121000
H	-4.370942000	-3.262694000	-0.308969000
C	-2.763920000	-1.847722000	-0.140883000
H	-1.988408000	-2.606095000	-0.185875000
N	1.094261000	0.740561000	0.134085000
N	-1.016009000	-0.231554000	0.048685000
O	1.286604000	-1.560719000	0.030051000
O	-5.691713000	1.123938000	0.032451000
S	-0.863749000	2.531133000	0.199766000
H	-6.605664000	0.796027000	-0.018921000
H	1.585245000	1.619180000	0.239995000
H	-0.432376000	-1.076710000	0.031075000

Z-matrix of the Ligand **C1.F**

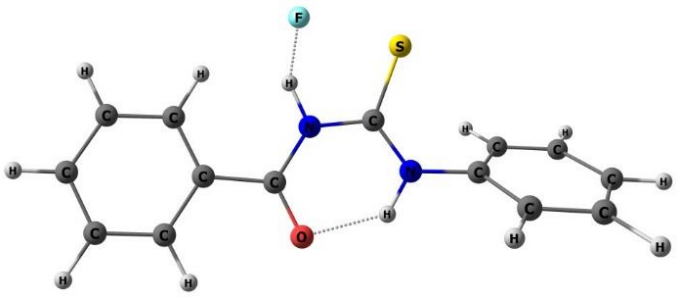

C	-5.741675000	-0.414017000	-0.013436000
C	-4.982123000	0.757740000	0.127165000
C	-3.583197000	0.700945000	0.104802000
C	-2.939016000	-0.542434000	-0.060218000
C	-3.703540000	-1.716423000	-0.199100000
C	-5.100246000	-1.652499000	-0.176505000
C	-1.458224000	-0.687432000	-0.090254000

N	-0.718118000	0.483307000	-0.009257000
C	0.646243000	0.594031000	0.014475000
N	1.403530000	-0.506063000	-0.086262000
C	2.837277000	-0.556578000	-0.064903000
C	3.602514000	0.210141000	-0.956364000
C	4.999823000	0.112155000	-0.920973000
C	5.626996000	-0.759029000	-0.017024000
C	4.851840000	-1.536299000	0.857302000
C	3.454497000	-1.433686000	0.838951000
O	-0.892512000	-1.809457000	-0.181813000
S	1.285167000	2.222825000	0.215971000
H	-6.825148000	-0.361853000	0.005232000
H	-5.475803000	1.714244000	0.255508000
H	-3.028157000	1.626665000	0.222059000
H	-3.188097000	-2.662356000	-0.322528000
H	-5.684922000	-2.559237000	-0.284471000
H	-1.148215000	1.445343000	0.080866000
H	0.874920000	-1.385978000	-0.149681000
H	3.116298000	0.864613000	-1.670887000
H	5.594924000	0.708635000	-1.603313000
H	6.708551000	-0.834651000	0.003308000
H	5.331399000	-2.212790000	1.555899000
H	2.847308000	-2.018489000	1.521941000
F	-0.934504000	2.920656000	0.265572000

Z-matrix of the Ligand **C2.F**

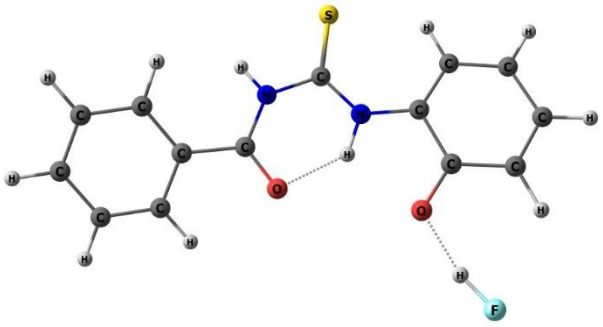

C	-3.270912000	-0.318288000	0.010571000
C	-3.851746000	-1.542321000	-0.367389000
H	-3.203804000	-2.352152000	-0.683738000
C	-5.241132000	-1.701267000	-0.326272000
H	-5.685794000	-2.644136000	-0.623680000
C	-6.057136000	-0.642492000	0.103028000
H	-7.133966000	-0.767027000	0.138538000
C	-5.479491000	0.573676000	0.499296000
H	-6.107120000	1.385056000	0.850094000
C	-4.089613000	0.738393000	0.453744000
H	-3.665648000	1.674914000	0.805046000
C	-1.783537000	-0.222192000	-0.054813000
C	0.093983000	1.472669000	-0.122168000
C	2.395264000	0.495969000	-0.007023000
C	3.229756000	1.621453000	0.009815000
H	2.806126000	2.613743000	-0.027325000
C	4.620511000	1.448831000	0.074077000
H	5.253534000	2.329528000	0.087340000
C	5.221993000	0.158650000	0.122260000
H	6.300943000	0.071083000	0.172654000
C	4.433069000	-0.971728000	0.105143000
H	4.846410000	-1.974080000	0.139639000
C	2.996209000	-0.843734000	0.039134000

H	2.908353000	-3.289799000	0.063008000
H	-1.887795000	1.842887000	-0.224173000
H	0.619318000	-0.503755000	-0.055569000
N	-1.249900000	1.063112000	-0.129605000
N	1.005024000	0.459711000	-0.060507000
O	2.213942000	-1.870015000	0.019050000
O	-1.049262000	-1.235737000	-0.060148000
S	0.380612000	3.150067000	-0.192460000
F	3.550336000	-4.022976000	0.095631000

Z-matrix of the Ligand **C3.F**

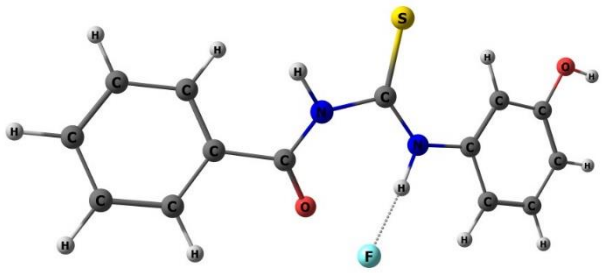

C	3.289230000	0.135483000	-0.149639000
C	3.781376000	-1.167605000	-0.362564000
H	3.104057000	-2.011641000	-0.460184000
C	5.158342000	-1.373389000	-0.504312000
H	5.539284000	-2.373322000	-0.677154000
C	6.042739000	-0.284491000	-0.436115000
H	7.109172000	-0.447961000	-0.546709000
C	5.549733000	1.015351000	-0.238252000
H	6.234103000	1.854690000	-0.192895000
C	4.174047000	1.229082000	-0.101186000
H	3.772652000	2.225353000	0.045915000
C	1.836783000	0.410535000	0.000549000
C	-0.330735000	-0.846912000	0.462783000
C	-2.492014000	0.376493000	0.050430000
C	-3.385170000	-0.687135000	-0.128745000

H	-3.071948000	-1.719030000	-0.071318000
C	-4.734203000	-0.399247000	-0.381833000
C	-5.205669000	0.918086000	-0.454695000
H	-6.254612000	1.124173000	-0.648885000
C	-4.295014000	1.970526000	-0.271219000
H	-4.643131000	2.995888000	-0.326262000
C	-2.947936000	1.713088000	-0.021950000
H	-2.247804000	2.531033000	0.113377000
N	1.075912000	-0.577903000	0.554698000
N	-1.099123000	0.238686000	0.298628000
O	1.380469000	1.532835000	-0.409740000
O	-5.567161000	-1.499018000	-0.552696000
S	-0.752172000	-2.493456000	0.574037000
H	-6.491078000	-1.245772000	-0.718981000
H	1.574083000	-1.378441000	0.928085000
H	-0.629722000	1.141728000	0.446065000
F	0.338516000	2.360379000	1.096783000

Z-matrix of the Ligand [Ni(**C2**)$_2$]

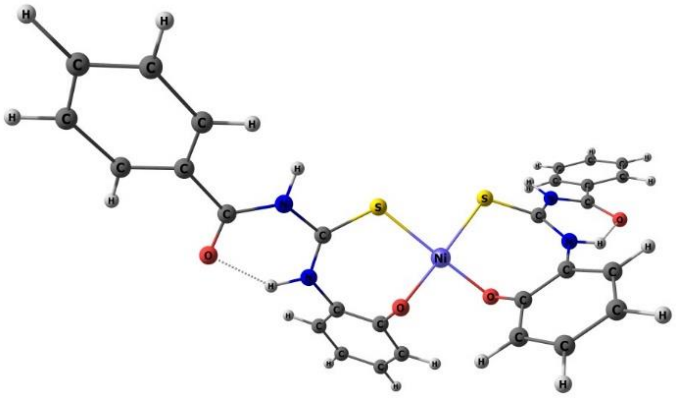

C	6.452574000	-1.721063000	0.477097000
C	7.766549000	-1.903639000	0.009873000
H	8.072354000	-1.402564000	-0.901724000
C	8.656071000	-2.717091000	0.720014000
H	9.665990000	-2.861339000	0.353171000

C	8.241524000	-3.342451000	1.906728000
H	8.931514000	-3.970602000	2.459555000
C	6.937320000	-3.145646000	2.386346000
H	6.622344000	-3.610910000	3.313377000
C	6.042074000	-2.337379000	1.674864000
H	5.052609000	-2.166866000	2.089449000
C	5.557075000	-0.840257000	-0.325816000
C	3.138025000	-0.298801000	-0.726120000
C	2.604763000	1.636532000	-2.195587000
C	2.913383000	1.966055000	-3.523759000
H	3.753979000	1.485585000	-4.016658000
C	2.130442000	2.902737000	-4.206059000
H	2.360329000	3.156829000	-5.234677000
C	1.039013000	3.503373000	-3.548079000
H	0.422623000	4.224059000	-4.076145000
C	0.740216000	3.183092000	-2.221507000
H	-0.100681000	3.622814000	-1.697051000
C	1.530085000	2.250848000	-1.510573000
H	3.874063000	-1.800848000	0.417881000
H	4.476997000	0.861042000	-1.639139000
N	4.189672000	-1.033111000	-0.160879000
N	3.467797000	0.723965000	-1.505677000
O	1.314001000	1.956969000	-0.206300000
O	6.004974000	0.022124000	-1.119815000
S	1.562777000	-0.977243000	-0.371040000
C	-6.452584000	-1.721039000	-0.477151000
C	-7.766583000	-1.903592000	-0.009983000
H	-8.072393000	-1.402573000	0.901642000
C	-8.656116000	-2.716953000	-0.720215000
H	-9.666054000	-2.861184000	-0.353417000
C	-8.241555000	-3.342245000	-1.906961000
H	-8.931554000	-3.970326000	-2.459857000

C	-6.937326000	-3.145464000	-2.386519000
H	-6.622339000	-3.610676000	-3.313572000
C	-6.042070000	-2.337287000	-1.674949000
H	-5.052585000	-2.166788000	-2.089488000
C	-5.557066000	-0.840334000	0.325849000
C	-3.138017000	-0.298893000	0.726135000
C	-2.604725000	1.636338000	2.195730000
C	-2.913292000	1.965829000	3.523923000
H	-3.753841000	1.485311000	4.016856000
C	-2.130363000	2.902536000	4.206201000
H	-2.360211000	3.156597000	5.234835000
C	-1.038993000	3.503236000	3.548178000
H	-0.422607000	4.223937000	4.076228000
C	-0.740251000	3.183000000	2.221583000
H	0.100601000	3.622768000	1.697095000
C	-1.530116000	2.250737000	1.510665000
H	-3.874059000	-1.800900000	-0.417905000
H	-4.476961000	0.860793000	1.639342000
N	-4.189665000	-1.033143000	0.160828000
N	-3.467757000	0.723759000	1.505845000
O	-1.314106000	1.956913000	0.206368000
O	-6.004943000	0.021962000	1.119954000
S	-1.562759000	-0.977291000	0.370902000
Ni	-0.000018000	0.686831000	0.000017000

Z-matrix of the Ligand [Cu(**C2**)$_2$]

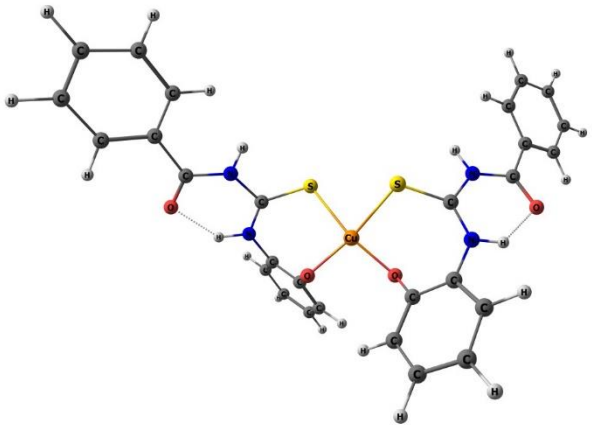

C	-5.969826000	-2.213077000	-0.585624000
C	-7.239526000	-1.994017000	-1.149620000
H	-7.676640000	-1.003889000	-1.085628000
C	-7.918307000	-3.043479000	-1.778446000
H	-8.893214000	-2.868764000	-2.219157000
C	-7.337516000	-4.320240000	-1.838377000
H	-7.863513000	-5.134323000	-2.325096000
C	-6.079247000	-4.546921000	-1.259528000
H	-5.636588000	-5.536024000	-1.289320000
C	-5.394756000	-3.497713000	-0.634147000
H	-4.439978000	-3.709883000	-0.161559000
C	-5.300799000	-1.050125000	0.065398000
C	-3.063069000	-0.211301000	0.828327000
C	-2.910569000	2.005973000	1.912524000
C	-3.397569000	2.489435000	3.135615000
H	-4.242157000	1.996611000	3.608613000
C	-2.785163000	3.590422000	3.742601000
H	-3.155051000	3.965297000	4.690260000
C	-1.678998000	4.197575000	3.115607000
H	-1.190383000	5.044155000	3.587568000
C	-1.202716000	3.723550000	1.891652000
H	-0.344888000	4.169924000	1.400981000

C	-1.824150000	2.627267000	1.247516000
H	-3.431117000	-1.922170000	-0.186424000
H	-4.609312000	1.015717000	1.139047000
N	-3.919685000	-1.131466000	0.212873000
N	-3.598043000	0.914228000	1.283991000
O	-1.427382000	2.189208000	0.035063000
O	-5.939282000	-0.040765000	0.448506000
S	-1.404154000	-0.757658000	0.974849000
C	5.969719000	-2.213246000	0.585556000
C	7.239375000	-1.994255000	1.149670000
H	7.676547000	-1.004149000	1.085721000
C	7.918029000	-3.043760000	1.778559000
H	8.892904000	-2.869108000	2.219367000
C	7.337157000	-4.320488000	1.838435000
H	7.863061000	-5.134602000	2.325201000
C	6.078931000	-4.547095000	1.259464000
H	5.636215000	-5.536174000	1.289217000
C	5.394566000	-3.497845000	0.634017000
H	4.439811000	-3.709927000	0.161344000
C	5.300784000	-1.050293000	-0.065547000
C	3.063057000	-0.211367000	-0.828433000
C	2.910700000	2.005964000	-1.912512000
C	3.397821000	2.489572000	-3.135497000
H	4.242415000	1.996758000	-3.608497000
C	2.785520000	3.590674000	-3.742374000
H	3.155494000	3.965663000	-4.689954000
C	1.679357000	4.197809000	-3.115356000
H	1.190828000	5.044492000	-3.587222000
C	1.202980000	3.723641000	-1.891495000
H	0.345174000	4.170014000	-1.400788000
C	1.824302000	2.627225000	-1.247471000
H	3.431093000	-1.922290000	0.186279000

H	4.609381000	1.015529000	-1.139211000
N	3.919656000	-1.131578000	-0.213017000
N	3.598097000	0.914132000	-1.284084000
O	1.427455000	2.189099000	-0.035072000
O	5.939340000	-0.041006000	-0.448714000
S	1.404105000	-0.757648000	-0.974926000
Cu	-0.000036000	0.958594000	0.000027000